FINAL REPORT

SUBMITTED TO THE NATIONAL SCIENCE FOUNDATION

by

University of Arizona

Long-term Spatial and Temporal Drought Frequency Analysis in Western United States Utilizing Tree Rings

Grant No. ATM 77-26189

Principal Investigator:

Charles W. Stockton
Laboratory of Tree-Ring Research
University of Arizona
Tucson, Arizona 85721

December, 1980

PREFACE

Studies of the "Long-Term Spatial and Temporal Drought Frequency Analysis in Western United States Utilizing Tree Rings" began on January 1, 1975 with the approval of Grant No. 74-24163 for one year in the amount of $40,500. A final technical report covering work accomplished during the funding period was submitted in July, 1976. Work continued throughout 1976 although additional funding was not provided.

Funding was again available under Grant No. ATM 76-08493 for $44,000 effective January 1, 1977. A progress report on work completed in 1976 through mid-1977 was submitted along with a renewal request covering two years. This request was approved and funded by Grant No. ATM 77-26189 beginning February 1, 1978. Funding for 1978 was $46,374 and was $49,457 for 1979 (through June 30, 1980).

The reports submitted in 1976 and 1977 provided details used in developing the mathematical relationships between tree-ring series and the Palmer Drought Severity Index along with results obtained for the period 1/1/75 - 6/30/77. Details of the methods or earlier results are not repeated here, but will be included in summary form.

The present report is divided into two major parts because of the rather divergent and somewhat definitive subject matter. Part I is concerned with the occurrence of drought and its persistence in different parts of the western United States. Part II provides a detailed discussion of the possible relationships between the occur-

rence of drought and solar variability, particulary the Hale Double Sunspot Cycle.

Several persons made significant contributions to the project. Those listed below deserve special recognition.

Dr. J. Murray Mitchell, NOAA, who first recognized the possible relationships between the periodic occurrence of drought area and solar variation. His participation, on a voluntary basis, made it possible for us to pursue this important aspect of the project.

David M. Meko, Graduate Student, for assuming major responsibility and leadership throughout the course of the project.

Irmgard Flaschka, Graduate Student, for her contributions in computer programming and development of the yearly maps showing the areas covered by drought of different intensities.

C. Larabee Winter, Graduate Student, for developing the Monte Carlo Simulations used in the solar variation aspect of the Study.

Submitted by

C. W. Stockton
W. R. Boggess
Laboratory of Tree Ring Research
University of Arizona
December, 1980

PART I : THE OCCURRENCE, DURATION AND SEVERITY OF DROUGHT PERIODS

INTRODUCTION

Droughts are a common and recurring meteorological phenomenon in all parts of the world. Although some regions are more drought-prone than others, few are immune. Severe or prolonged droughts affect two basic and essential human needs - food and water. They are of concern, therefore, to all segments of society on a world-wide basis. Knowledge of the occurrence, duration, persistence and severity of drought is an essential element in both land use and water resources planning.

Drought is difficult to define in specific terms, since it does not mean the same thing to all people. Basically, drought is a meteorological anomaly related to specific patterns of atmospheric pressure and circulation and is characterized by prolonged periods of moisture deficiencies. From a more practical standpoint, "agricultural drought" occurs when the moisture shortages have an adverse effect on crop and livestock production. This, in turn, may be followed by "hydrologic drought", when streamflow is reduced to the point where lakes and impoundments begin to dry up or groundwater levels are lowered due to lack of recharge. These two forms of drought are obviously related and are likely to occur in the order listed above. Droughts may be characterized by three factors - duration, severity and recurrence interval. Duration and severity can be directly assessed but the recurrence, or time between drought periods is more difficult to establish. An approximate 22-year periodicity for major droughts affecting the northern hemisphere, especially the North American continent, has been suggested by a number of investigators.

(Willett, 1965; Palmer, 1964; Thompson, 1973; Roberts, 1975). However, the meteorological data base is not long enough to verify the cyclic aspects of drought.

In the absence of instrumented data, it is necessary to turn to some proxy source that may reflect past climatic conditions. The most commonly used proxy data sources include layered ice cores; pollen profiles developed from bog, swamp or lake sediments; stream stratigraphy and morphology; and tree rings. The first three sources can generally be extended farther back in time than tree rings, but they cannot be precisely dated and lack the capacity to preserve high frequency (short term) variations. In contrast, tree rings can be dated to the year of formation and preserve both high and low frequency variations.

Data from tree rings represents the best developed method for reconstructing past climates. This approach, known as Dendroclimatology, has been largely developed at the Laboratory of Tree Ring Research, University of Arizona, and uses the width and other characteristics of annual growth rings as climatic indicators. Trees growing on sites where conditions for growth are marginal are particularly sensitive to various aspects of climate, especially the availability of moisture. Comparatively wide rings are produced in wet years and narrow rings when moisture is limiting. We have used the techniques developed at the Tree Ring Laboratory to reconstruct some 360 years of drought history, essentially for that part of the United States west of the Mississippi River. Results and implications of these reconstructions are discussed here.

DATA BASE

Meteorological

The Palmer Drought Severity Index (Palmer, 1965) was used to indicate the severity and duration of drought periods. This index (PDSI) was developed by W. C. Palmer of the old U. S. Weather Bureau and is based on an empirical water balance approach. The Thornthwaite method (Thornthwaite, 1948; Thornthwaite and Mather, 1955) of computing Potential Evapotranspiration from readily available precipitation and temperature data forms a basis for calculating the climatic demand for water and the subsequent development of the PDSI. The PDSI for a given month is partly determined by the index value for the preceding month and partly from moisture received during the month in question. A moisture anomaly is defined as the departure from that expected under "normal" conditions. The expected available moisture is calculated by the water balance approach and takes into account accumulated soil moisture levels and estimated evapotranspiration.

Maps showing PDSI values for the United States appear monthly in the Weekly Weather and Crop Bulletin published by the National Oceanic and Atmospheric Administration. An example is shown by Figure 1. A given PDSI value indicates the same degree of drought from one location to another. The PDSI is also an integrative index of moisture conditions similar to the response recorded by tree ring series. From a hydrologic standpoint the PDSI is a desirable index for slower response systems such as fluctuations in groundwater levels and for storage in large reservoirs.

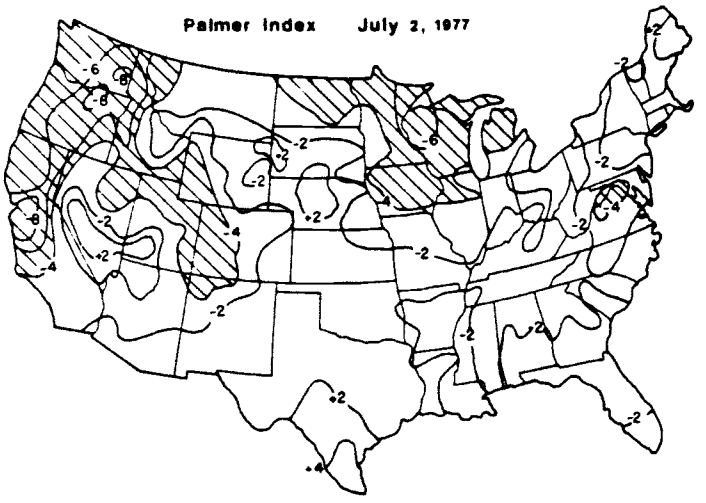

Figure 1. Map of Palmer Drought Severity Index for July, 1977 (redrawn from Weekly Weather and Crop Bulletin, 1977)

PDSI data for the period 1931-1970 were obtained from the National Climatic Data center in Asheville, North Carolina, and consisted of monthly values for each of the climatic divisions in the western United States. The study area included 204 climatic divisions. These were grouped into 40 regions using the rainfall classification system of Trewatha (1961) to define their boundaries. Regional PDSI series were calculated as the arithmetic mean of the PDSI of the divisions within each region.

Tree Rings

Most of the tree-ring data used were not specifically collected for this study but existed in the files of the Laboratory of Tree-Ring Research. We utilized data grids of 40 (S-40), 50 (S-50) and 65 (F-65) tree ring sites selected on the basis of replication, location and sensitivity to climatic variations (Figure 2 - B, C, D). Grids S-50 and F-65 dated back

to A. D. 1600 but their locations were largely west of the Great Plains. Grid S-40 contained fewer and only dated back to A. D. 1700 but included some locations on the eastern border of the Plains Region. The combination of all three grids provided maximum spatial and temporal coverage. Trees sampled included species of pine (Pinus, spp.). Oaks (Quercus, spp.) and Douglas Fir (Pseudotsuga Menzessi).

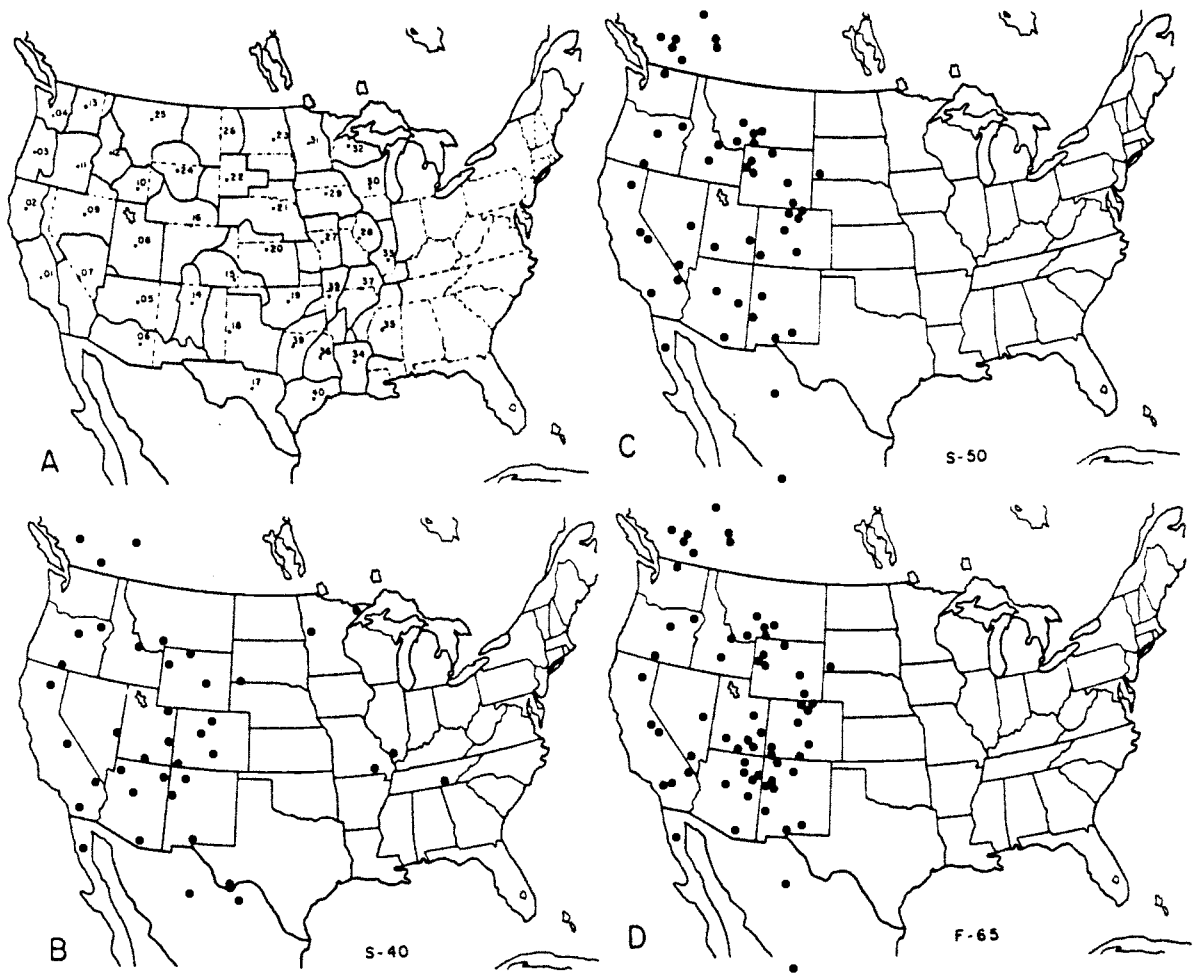

Figure 2. Domain of drought analysis on which this study is based. (A) : Areas with solid boundaries and interior numbers identify the 40 climatic regions in which PDSI was observed or reconstructed. (B): Spatial distribution of tree-ring data sites (grid S-40) used in reconstructing PDSI to 1700 A. D. (C): Spatial distribution of tree-ring sites (grid S-50), used in reconstructing PDSI to 1601 A. D. (D): Spatial distribution of tree-ring sites (F-65) used in reconstructing PDSI to 1600 A. D.

RECONSTRUCTION TECHNIQUES

Since drought was to be constructed from annual tree-ring indices, while the regional PDSI series consisted of monthly values, it was necessary to derive some annual measure of drought that might be strongly related to tree-ring growth. The July PDSI was chosen for the following reasons: annual tree growth as reflected in ring widths is essentially completed by the end of July; July PDSI reflects, to some degree, the moisture conditions of the prior spring and winter - these conditions are relatively important to most of the tree species used in this study; major droughts from 1931-1971 tended to reach peak intensity in July or August; July PDSI is particularly important in the growth and yield of agricultural crops; and July is generally the peak month for water use, both for irrigation and human consumption.

An empirical orthogonal function analysis was performed on both the PDSI and tree-ring data grids to define a smaller number of variables accounting for most of the spatial and temporal variability in both series (Fritts, 1976). Empirical orthogonal function analysis enables fields of highly correlated data to be represented adequately by a smaller number of orthogonal functions (eigenvectors) describing the patterns in space, and corresponding orthogonal amplitudes as they vary in time. Kutzbach (1967) provides a detailed explanation of the mathematical procedure necessary to define the functions and their amplitudes.

Empirical orthogonal functions (eigenvectors) of the PDSI were computed from the 40 observations of July PDSI (1931-1970) in the 40 regions. The analysis indicated the 40 original spatial patterns of PDSI could be

represented quite well by the first five eigenvectors (explaining 75% of the variance). The first eigenvector accounted for 38 percent, the second for 17 percent, the third for 11 percent and the remaining fourth and fifth together for about 10 percent of the variance.

A similar analysis was performed on the 264-year record (A. D. 1700-1963) of tree-ring indices for the 40 sites of Grid S-40 and for the 365-year record (1600-1963) for Grids S-50 and F-65. The first 10 eigenvectors accounted for about 60 percent of the variation with the first five of these representing nearly 50 percent of the total variance. The tree-ring record overlapped the PDSI record for the years 1931-1963, and these years were used to derive a transfer function for reconstruction (Fritts, 1976). The approach to reconstructing the long-term drought record consisted of deriving relationships to predict PDSI amplitudes from tree-ring amplitudes using canonical analysis (Fritts, et. al., 1971; Blasing, 1978). For Grid S-40 a total of 6 amplitudes were used, accounting for 45 percent of the total variance; in the S-50 grid case, only the first two amplitudes were used, but they were entered into the transfer function such that drought at the time t was compared with tree-ring data over the times t+1, t, and t-1, for a total of 6 variables. The first two amplitudes account for 32% of the total variance in the 50 station tree-ring data grid over the period A.D. 1931-1962. The information for all grids is summarized in Table 1 (A-C).

Canonical analysis was used to derive a matrix of least squares coefficients to predict amplitudes derived from the first five PDSI eigenvectors from the amplitudes of tree-ring series eigenvectors. The resulting

TABLE 1

DROUGHT AREA RECONSTRUCTIONS

GRID	(A) TREE-RING INDICES				(B) DROUGHT INDICES (PDSI)			
	Period of Record	Data Points	EVs# Retained	Variance Explained	Period of Record	Data Points	EVs# Retained	Variance Explained
S-40	1700-1962	40	6	45%	1931-1970	40	5	75%
S-50	1600-1962	50	2	31%	1931-1970	40	7	83%
F-65	1600-1962	65	3	41%	1931-1970	40	5	75%

DAI FAMILY	(C) CANONICAL "BRIDGE"[1]		(D) DAI VARIANCE EXPLAINED*			
	Terms Retained	Variance In Common*	PDSI LIMIT <-1	<-2	<-3	<-4
S-40	5	64%	72%	72%	74%	73%
S-50	6	56%	67%	76%	79%	75%
F-65	5	65%	69%	70%	79%	74%

*In overlap period 1931-1962 (32 years)
#EVs = Eigenvectors

PDSI = Palmer Drought Severity
DAI = Drought Area Index

1. The maximum number of "terms retained" can not exceed the smallest number of variables in either set. The variables for the tree-ring set included the amplitudes lagged so that the PDSI amplitudes at time t are compared with those from the tree-ring set at times t and t + 1 (Grids S-40, and F-65) and t , t + 1, and t - 1, (Grid S-50).

transfer function explained about 64 percent of the variance of the PDSI amplitude series during the calibration period (1931-1963) for Grid S-40 and about 56 percent for Grid S-50 and 65 percent for Grid F-65.

This same transfer function was then applied to the 1700-1962 and 1600-1963 tree-ring amplitude series and in this manner the amplitudes of the PDSI were reconstructed back to 1700 (Grid S-40) and 1600 (Grids S-50 and F-65). Reconstructed values of the PDSI series were then obtained by multiplying the matrix of predicted PDSI amplitudes by the matrix of appropriate PDSI eigenvectors.

Time series of July PDSI were reconstructed for each of the 40 climatic regions using the above procedures. Drought Area Indices (DAI) were then calculated by tabulating the total number of regions in a given drought class for each year. The resulting DAI series are approximate annual measures of the areal extent of a given severity of drought. For example, the DAI series for PDSI $\leq$ -2 is simply an annual frequency count of the number of regions reconstructed for PDSI $\leq$ -2.0. A total of 12 DAI series was reconstructed - one each for PDSI $\leq$ -1, $\leq$ -2, $\leq$ -3 and $\leq$ -4 from each of the three tree-ring data grids.

The actual and reconstructed DAI series for the calibration period agree reasonably well, with the longer term variation especially well duplicated. The percent variance explained (r^2 x 100) by the various DAI reconstructions were generally above 70 percent and similar results were obtained for a given drought class from the different tree-ring grids.

The DAI values do not provide information on the actual geographic areas within the western United States affected by drought. To accomplish this purpose, yearly maps for the 1700-1962 period were computer generated to show the approximate areas covered by droughts of different intensity. The S-40 data grid was used for these maps because of its greater spatial coverage. An example is shown for A. D. 1846, one of the drier years during the reconstruction period (Figure 3).

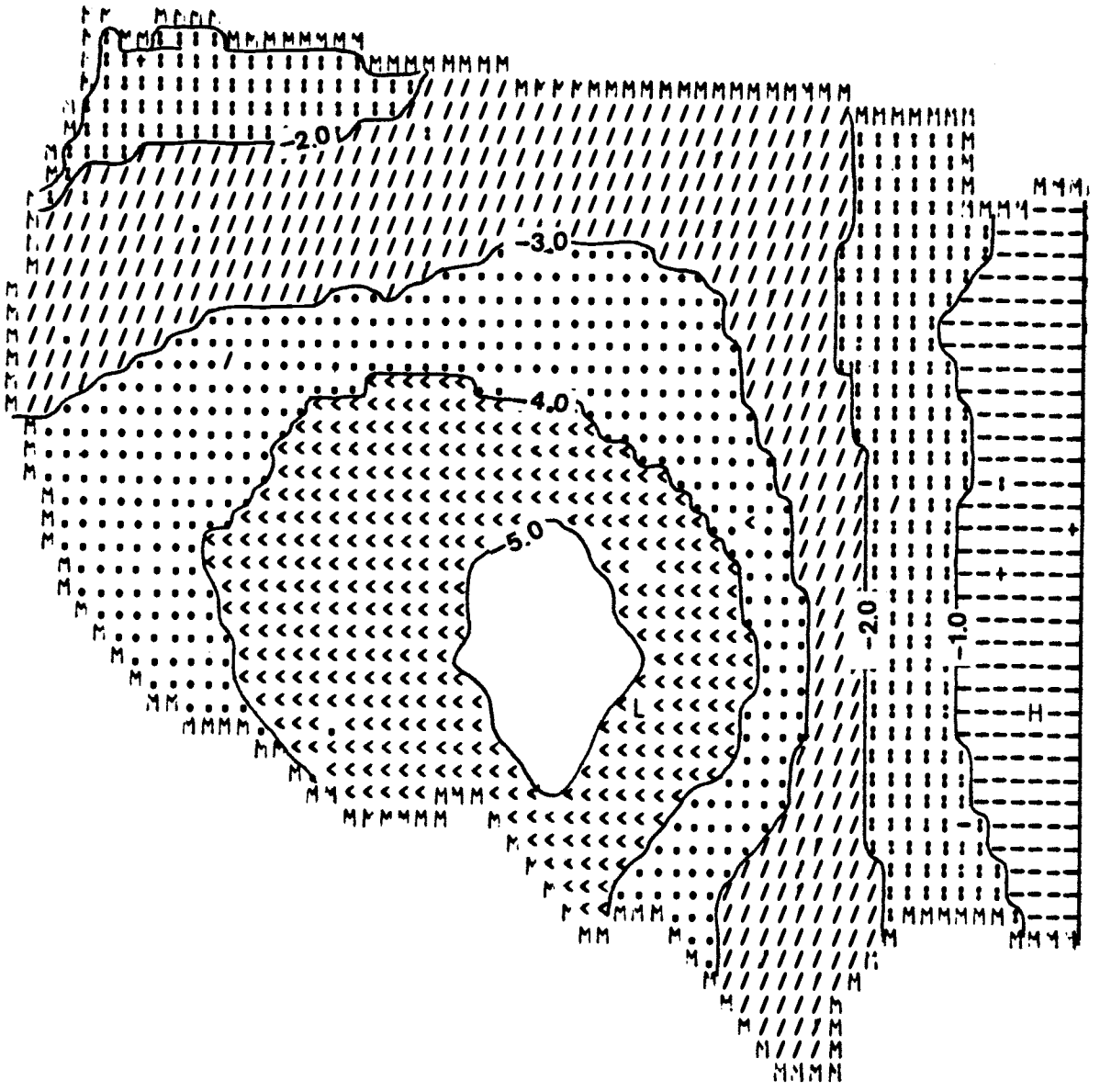

Figure 3. Computer generated map showing areas covered by drought of various intensities for A. D. 1847.

DROUGHT CHARACTERISTICS

Occurrence

A time series for the period A.D. 1700-1962 showing the number of regions with PDSI $\geq$ +1.0 and $\leq$ -1.0 is presented by Figure 4. The significant point illustrated here is the rhythmic alternations of wet and dry periods. This periodicity indicates that the area covered by drought equalling or exceeding PDSI -1.0 in severity, tends to reach a maximum at intervals of approximately 22 years. This 262 year reconstructed record confirms the suspected 22-year cycle mentioned earlier. In recent years, for example, severe droughts have affected the western United States in the mid-30's, mid-50's and mid-70's.

With regards to the likely occurrence of dry periods, we emphasize that out results are based on the area covered by drought. Thus there is no assurance that the approximate 22-year periodicity will hold for any specific geographic location or area within the western United States. This point is illustrated by the PDSI maps for 1934, 1936, 1954, and 1956 as shown on Figure 5. These maps were prepared from actual data supplied by the National Climatic Center in Asheville, North Carolina. Note the shifting areas affected by drought, both within and between periods. The same shifting patterns were observed throughout the period of reconstruction.

Duration and Severity

The percentage of the 40 climatic regions west of the Mississippi River with a PDSI of -2 or less for intervals of 1, 2, 3, 5 and 10 years is shown in Table 2 (based on Grid S-50, A.D. 1600-1972). Note that the

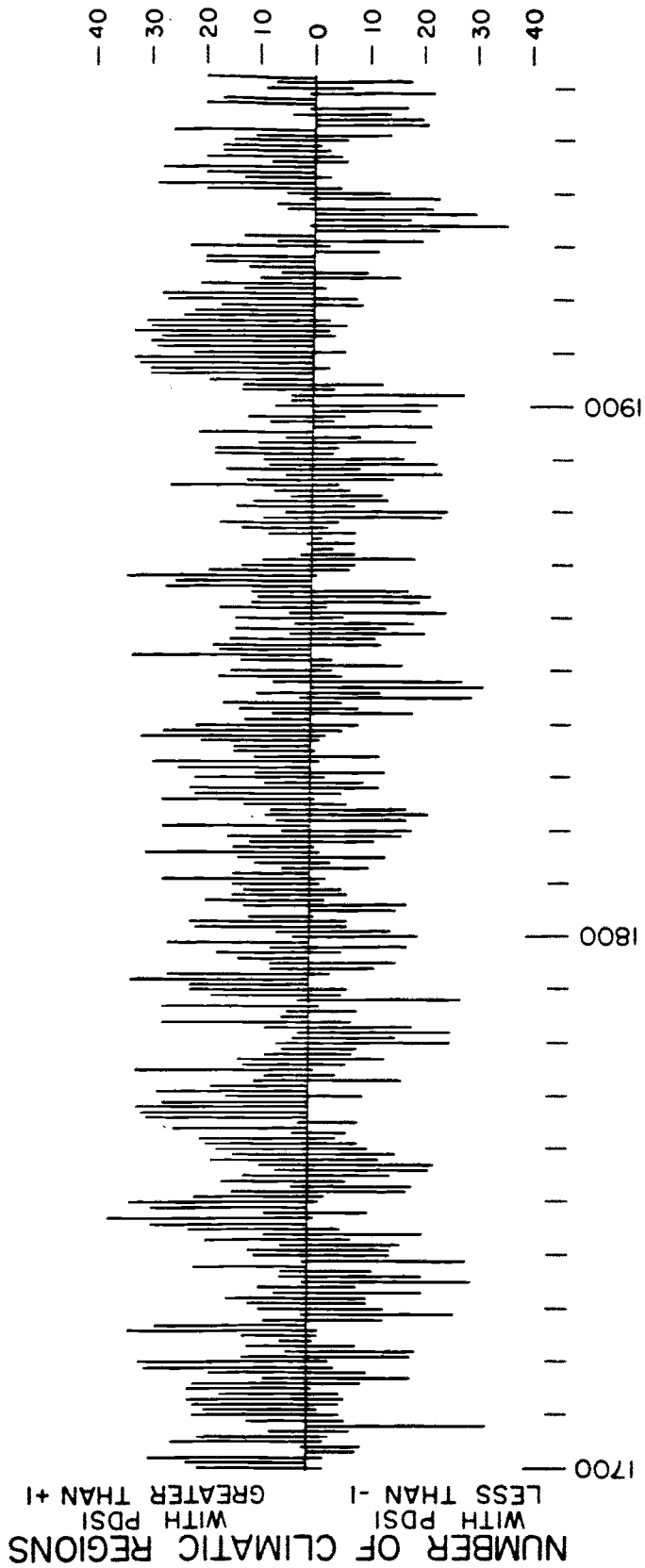

Figure 4. Long-term reconstructed Drought Area Index for drier than normal (PDSI $\leq$ -1.0) and wetter than normal (PDSI $\geq$ +1.0) categories, A.D. 1700-1962 from Grid S-40.

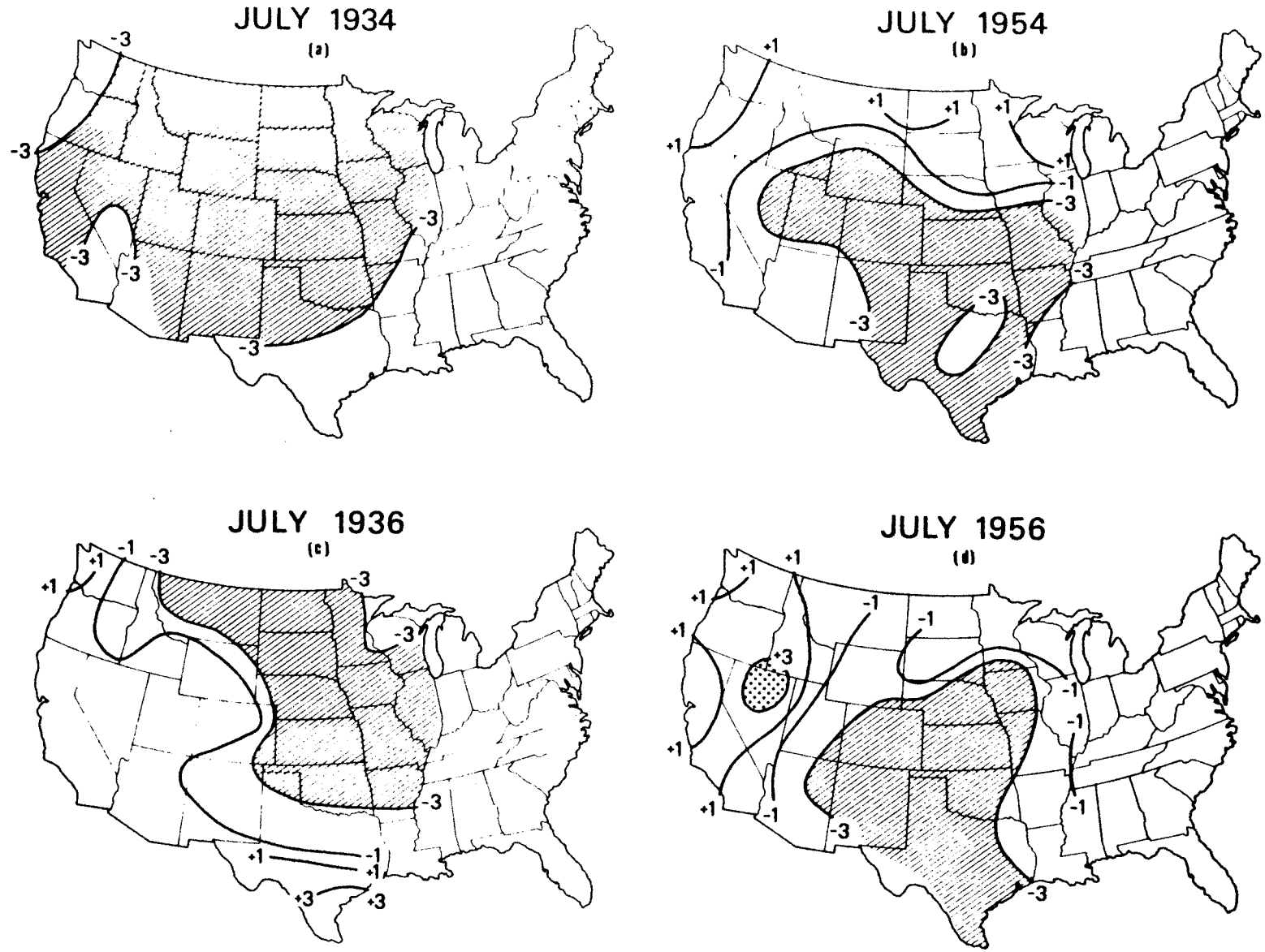

Figure 5. The four driest Julys (1934, 1936, 1954, 1956) in the period 1931-1970, as indicated by regionally averaged Palmer Drought Severity Index (PDSI). Shaded area indicates PDSI $\leq$ -3.0.

most widespread drought during the entire period of reconstruction occurred in the 1930's. This drought period actually began in 1931 and in the most severely affected areas, the so-called "dust bowl", was not broken until 1940. The economic losses and social upheaval caused by this great drought are well documented. For longer periods of time the driest years were as follows: 20 years: 1845-1864; 25 years: 1841-1865; 50 years: 1708-1757; 75 years: 1715-1789.

In contrast to the drought periods which have occurred during the 362 years of reconstruction, the wettest 1, 2, 3, 5, and 10 years are all in the present century.

TABLE 2: Percent of total area with PDSI -2.0 or less for 1, 2, 3, 5, and 10 year periods.

1 year		2 year		3 year		5 year		10 year	
Year	%	Year	%	Year	%	Year	%	Year	%
1934	78	1863-64	56	1863-65	52	1933-37	38	1931-40	24
1632	68	1933-34	54	1934-36	50	1932-36	36	1930-39	24
1735	68	1782-83	53	1630-32	44	1861-65	35	1856-65	23
1847	68	1847-48	51	1781-83	43	1934-38	32	1857-66	23
1626	65	1631-32	48	1933-35	42	1844-48	32	1842-51	22

Probability of Occurrence

We have used the individual time series for each region to calculate the probability of occurrence of drought for PDSI $\leq$ -1 and $\leq$ -2 based on actual data from 1930-1962 and on reconstructed values for 1700-1962 (Grid S-40) and 1600-1962 (Grid S-50). Data for 1931-1962 are plotted as lines of equal probability on Figure 6.

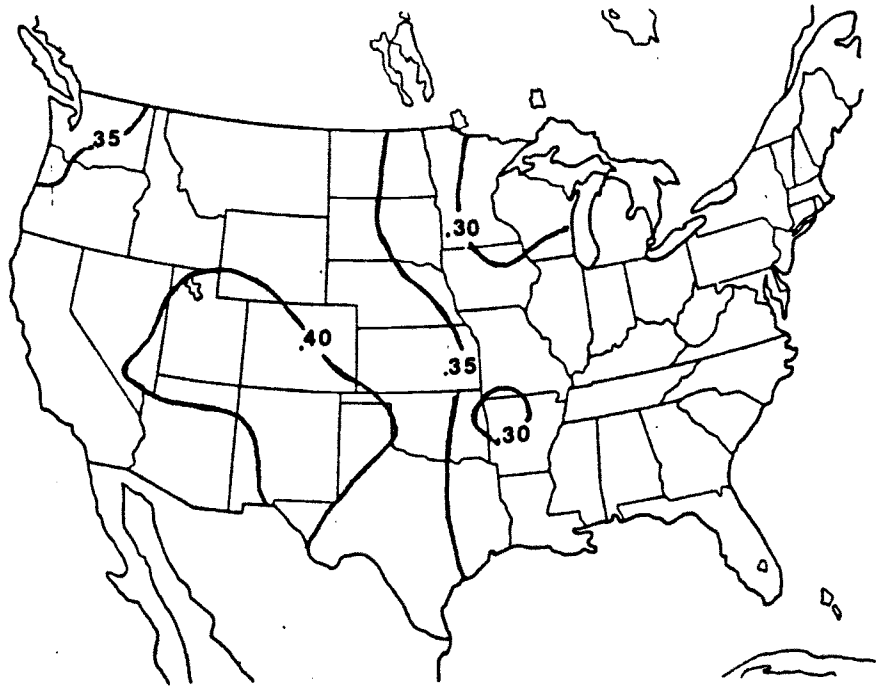

Figure 6. Map of probability of occurrence of July drought with PDSI $\leq$ -1. Meteorological data for 1931-1962 used in computations.

It is evident that for the majority of the western United States, the probability is greater than 35% that any given July will have a PDSI $\leq$ -1. The area of greatest probability lies over Utah, Wyoming, Colorado, New Mexico, Arizona, and west Texas. A map for the same period computed from the S-40 tree-ring grid is comparable, showing most of

of the West with a probability of at least 25% of any July having a PDSI $\leq$ -1 and the area of greatest probability being in Montana, Idaho, Wyoming, Colorado and Utah. Figures 7 and 8 are similar to Figure 6, except that they are computed from tree-ring data for the period 1700-1962 (Grid S-40) and 1600-1962 (Grid S-50). Figures 9 and 10 show the results for PDSI $\leq$ -2.

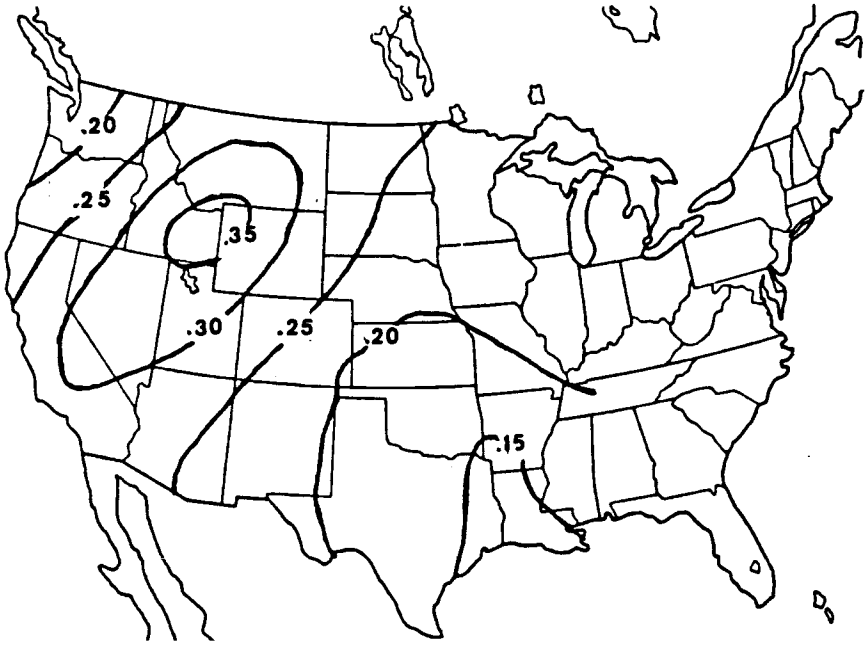

Figure 7. Map of probability of occurrence of July drought with PDSI $\leq$ -1. Tree-ring data for period 1700-1962 used in reconstruction of drought area.

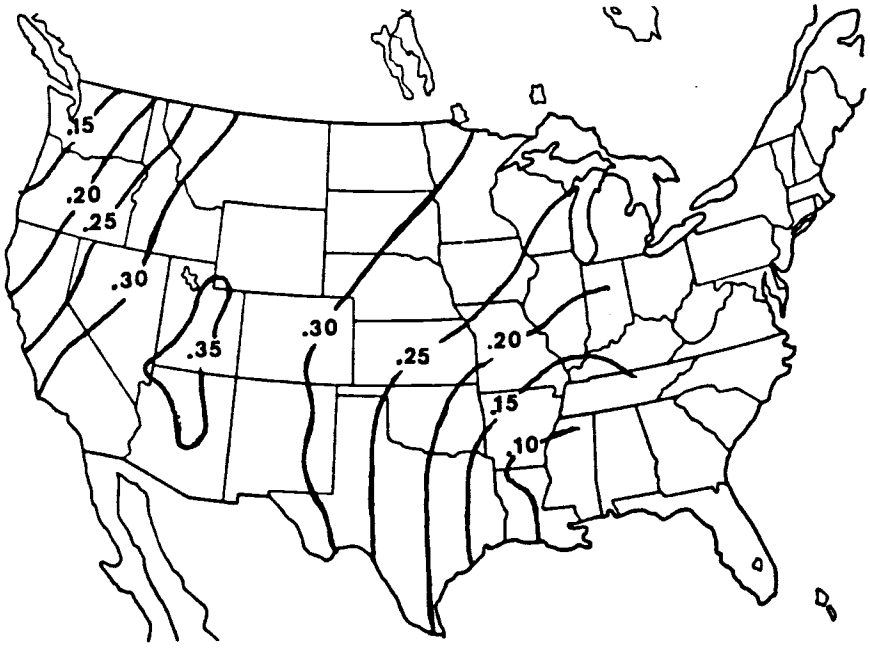

Figure 8. Same as Figure 7 except tree-ring data for period 1600-1962 used in reconstruction of drought data.

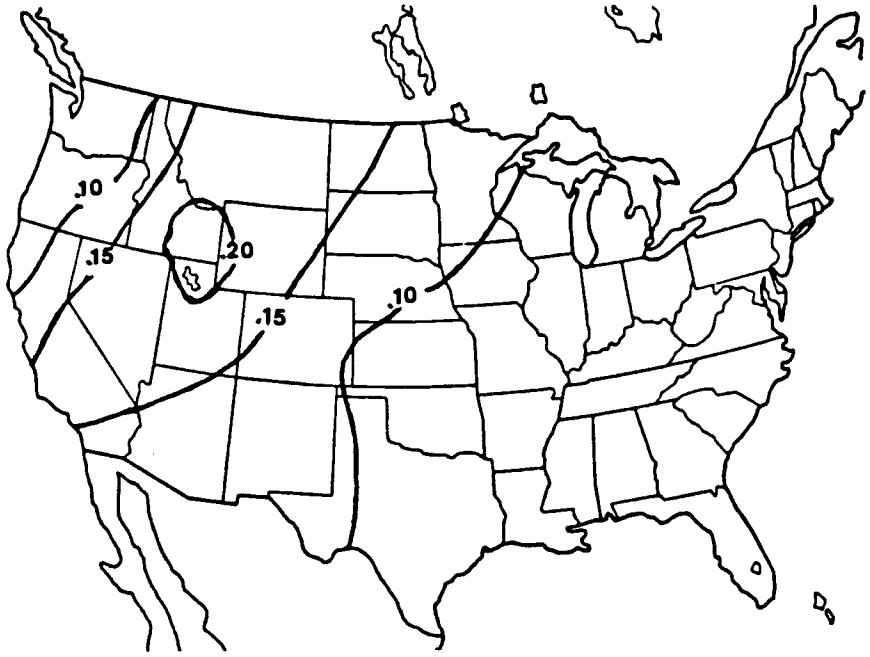

Figure 9. Map of probability of occurrence of July drought with PDSI $\leq$ -2. Tree-ring data for period 1700-1962 used in reconstruction of drought area.

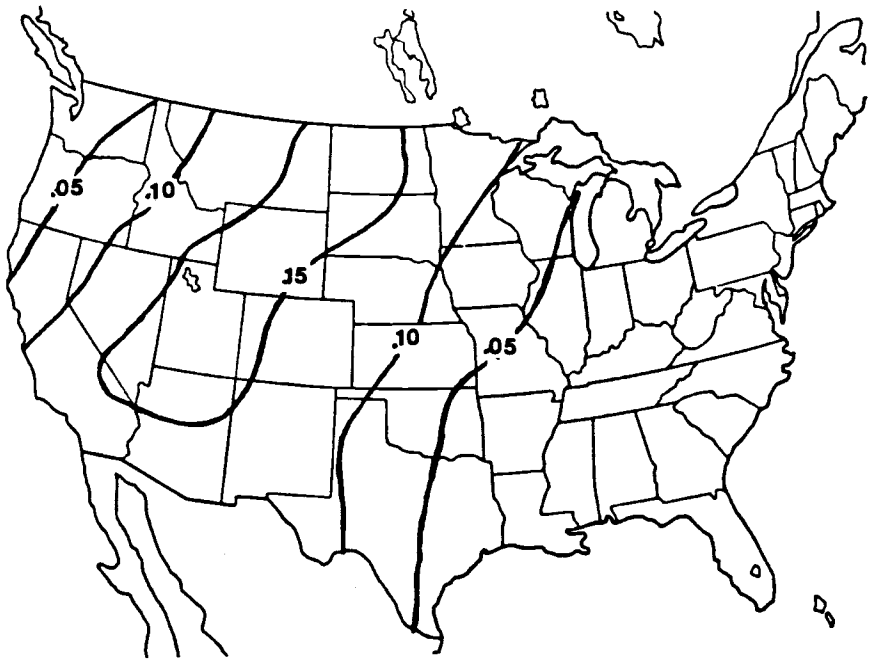

Figure 10. Same as Figure 8 except tree-ring data for period 1600-1962 used in reconstruction of drought area.

The area enclosed by the .3 probability isoline is diminished considerably for the S-40 grid, while for the S-50 grid it includes a rather large northeast-southwest trending portion of the western United States. (Note that the S-50 grid extends back to 1600, whereas the S-40 grid goes back to 1700; but the space coverage is greater for the S-40 grid). Both data grids show the region of maximum drought probability extending in a rather large band from the southwest toward the northeast over the western United States, with the probabilities diminishing in a rather sharp gradient towards the northwest and southeast.

Persistence of Drought

Persistence is an important attribute of both meteorologic and hydrologic time series that attempts to define and quantify the likely occurrence and duration of above or below normal conditions - e. g. wet vs dry years; high vs low flows. Our results suggest a greater persistence of dry as opposed to wet years. This is indicated by the highly skewed distributions when the frequency distribution of drought areas per unit of time was calculated for PDSIs of ≤ -1, ≤ -2 and ≤ -3. This agrees with pioneering work in this country by Hoyt and Langbein (1944) who investigated relationships between climate and streamflow. Their conclusions were upheld later by Julian (1970) based on analyses of a network of runoff and precipitation stations.

The classic work in quantifying climatic persistence in hydrologic time series was that of H. E. Hurst, a hydrologic engineer working on reservoir design for the Nile River in Egypt. The very long records for the Nile provided a unique opportunity for Hurst to investigate the occurrence and persistence of high and low flows.

Based on these studies, Hurst (1951) determined that the maximum and minimum of the cumulative departures from the mean provided a useful statistic for measuring long-term fluctuations in geophysical time series. This relationship may be expressed as

$$\frac{R}{S} = \left(\frac{n}{2}\right)^k$$

where:

R = range (maximum - minimum) of cumulative departures from the mean of a time series

S = standard deviation

n = length of record in years

k = coefficient which Hurst found to range from 0.46 to 0.96 with a mean of 0.726.

It is important to note that the theoretical value of k is 0.5 for a series of purely random events, and those with short memory (e.g. first order Markov Processes). The considerable departures of k from 0.5 noted above has been the subject for much discussion among theoreticians, especially since the relationships were developed empirically. Later, Hurst (1957) and Hurst et. al. (1965) extended his investigations to other time series occurring in nature, including long-term tree-ring records from the western United States. These additional studies confirmed his Nile River Results.

It now seems apparent that Hurst's work demonstrated the fact that $k > 0.5$ because of the climatically induced low frequency signal (which was his original conjecture) and furthermore that climate is not a random function of time. These two points are extremely important in water resources planning.

Hurst's k was computed for each of the 40 climatic regions based upon the tree-ring derived PDSI records. Utilizing the calculated k values, lines of equal k (iso-k) were constructed for the western two-thirds of the country; the S-50 grid was used in this analysis, so that the longest period is 363 years. Iso-k maps for 50 and 100-year increments were also developed to evaluate the change with record length over the period 1600-1962. The iso-k map for 50 year increments is shown in Figure 11(a). This map is interpreted as showing the persistence in the PDSI series with the greater values representing the regions of highest persistence in drought. Figure 11(b) shows a comparable analysis, but for 100 year increments. Figure 11(c) is the same but for the entire 363 year record. All three maps show a decrease in drought persistence in the northwestern and southeastern regions of the United States. The regions of greatest persistence (highest k values) varies somewhat as n changes, but in general includes a rather wide band extending from the northwest to the southeast over the western United States. The values represent averages for the indicated intervals, except for the 363 year period which represents a single value. In all three cases, the values decrease in the northwest-southeast direction. As expected, the values decrease as n increases. In all three cases, the values are greater than .5, suggesting that the occurrence of drought as reflected by the PDSI is not a random phenomenon, although for the 50 year intervals it approaches .55 in the southeastern region.

In summary, these maps indicate that long-term persistence in drought is greatest in the central and northern Great Plains Regions, northern Rocky Mountains and Great Basin and the Colorado River Basin.

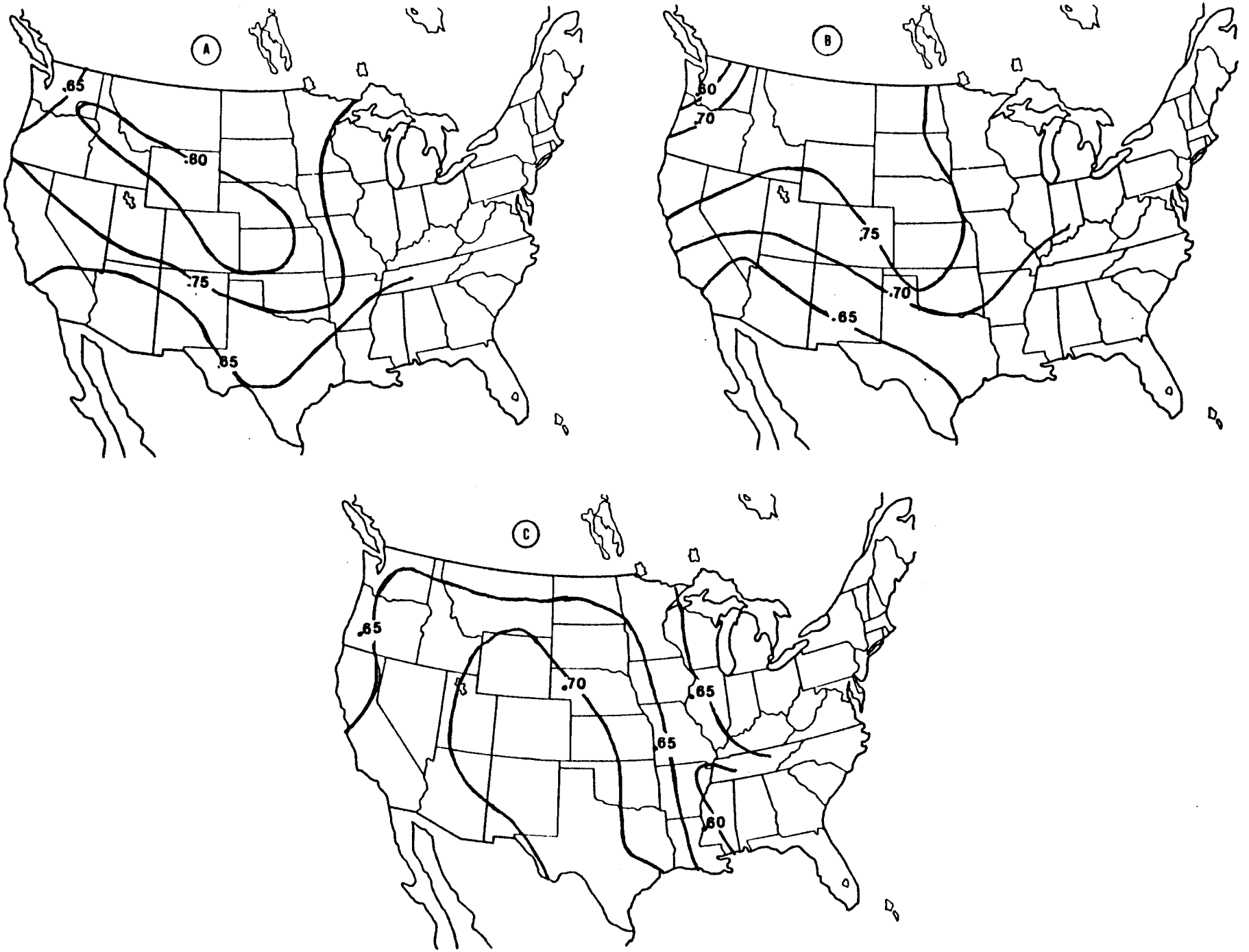

Figure 11. Maps showing regions of most persistent drought occurrence as expressed by Hurst's k. Larger values indicate greater persistence. (a) is based on 50 year increments; (b) is based on 100 year increments and (c) on the 363 years of record (1600-1962).

Drought is least persistent in the extreme northwest and southwestern portion of the nation. This is in agreement with earlier stated results and the expectation that the regions of least likely long-term drought persistence are the northwest and southeast.

One of the reservations frequently expressed concerning results based on tree-ring data is the effect of biological components in the series. The biological trend (decreased growth due to age) is removed by fitting a predetermined curve to the data and removing the change due to age by converting measured ring widths to indices. Short-term effects are removed by modeling techniques used in the transfer function analysis. The techniques utilized in both cases are explained in considerable detail by Fritts (1976). However, the question still remains as to the influence of biological factors and/or their removal on values of Hurst's k. For this reason, a 5400 year sequence of data from bristlecone pine has been analyzed for both raw ring widths and for the indices. This was done for 100 year, 500 year and 1000 year increments. The changes in k for the raw ring widths, for the indices as a function of time, and for all three increments are shown in Figures 12 (a,b,c). For the 100 year increments, little change results; for 500 year increments, the trend (due to growth) is apparent with the average difference being .10, while the average k for the indices differed by -.10. For 1000-year increments, the average difference is also near .10. So, based on this limited sample, it appears that by extracting the growth curve from the basic tree-ring data, the average k value is reduced by .10, when the increment upon which the k value is based is near 1/4 the length of the original tree-ring data series. However, it also appears that the k value

decreases in time for the raw ring width series corresponding to the expected trend based on the growth curve. In addition, the absolute values of k appear to be more near the mean population values of .73 as determined by Hurst, after the raw ring widths are converted to indices. Consequently, based on biological reasons and statistical reasoning, it appears that the value of k as determined from tree-ring data is not adversely affected by removing the growth trend.

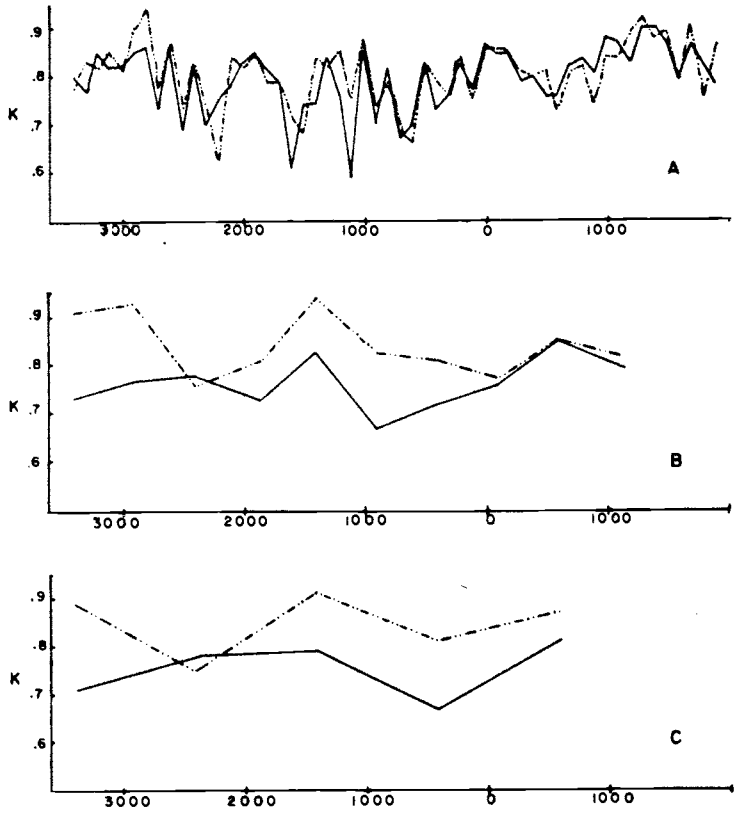

Figure 12. Change of Hurst's k with time for a 5400 year length Bristlecone pine series. (A) is for 100 year increments; (B) for 500 year; and (C) for 1000 year increments. Dashed line shows the values computed for ring width, solid line after conversion to indices.

REGIONAL DROUGHT CONSIDERATIONS

The methods described for large-scale drought reconstructions were applied to southern California to determine whether the same approach could be used to reconstruct drought for a much smaller area. Results indicate that regional reconstructions are both practical and feasible. The study is briefly summarized here as details were included in the previous progress report and the results have also been published (Meko, Stockton and Boggess, 1980). Judging from the number of requests for reprints, this study has created considerable interest.

We utilized tree-ring data from 8 sites located in southern California and northwestern Mexico along with climatic information from Los Angeles, San Diego and Riverside (Figure 13).

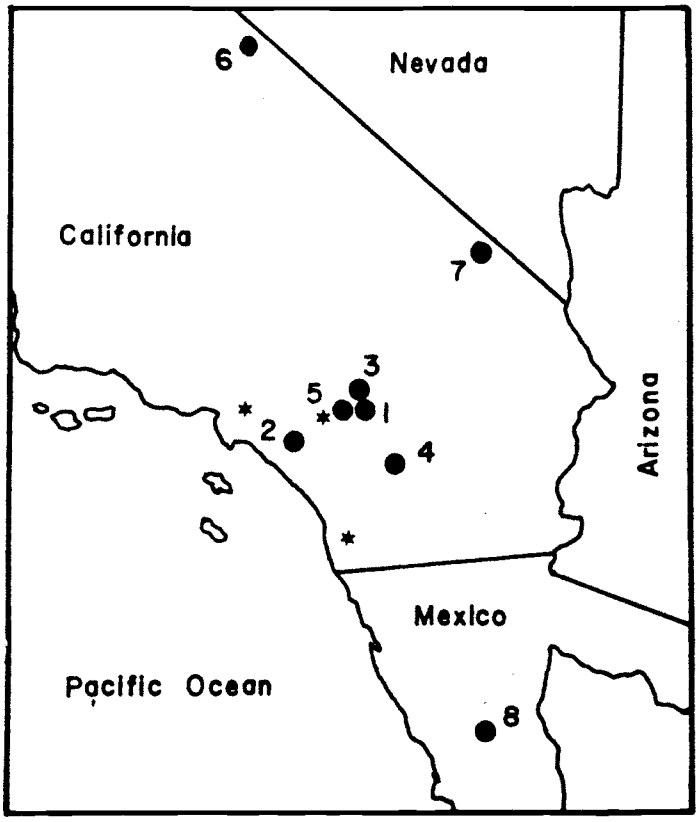

Figure 13. Map showing locations of tree-ring sites (dots) and weather stations (stars) used in reconstructing drought in Southern California.

The overlapping tree-ring and meteorological data provided a calibration period of 82 years. The number of years reconstructed at drought levels of PDSI $\leq$ -1.5 (moderate), $\leq$ -2.6 (severe) and $\leq$ -3.5 (extreme) for discrete 50 year intervals and for the 1950-1963 period are listed below.

	PDSI ≤ -3.5	PDSI ≤ -2.6	PDSI ≤ -1.5
Period		Number of Years	
1700-1749	4	5	8
1750-1799	5	7	10
1800-1849	6	8	14
1850-1899	6	8	14
1900-1949	2	4	11
1950-1963	3	3	6

Droughts at all three levels were most frequent in the two periods making up the 19th century. Extreme droughts (PDSI $\leq$ -3.5) were relatively rare in the first half of the twentieth century but have become more frequent since 1950. In three years during 1950-1963 reconstructed PDSI was below -3.5, and actual PDSI was below -4.0 again in 1970 and 1972. Evidence so far therefore suggests that the current half-century may well turn out to be the driest such period since A.D. 1700.

An important problem to water resource planners and others is the likelihood of droughts lasting several years. Only in 1863-64 and in 1898-99 were years reconstructed back-to-back in extreme drought (PDSI $\leq$ -3.5). Droughts lasting three years were evidently rare over the study period, with no three-year droughts at the extreme level, only one at the severe (PDSI $\leq$ -2.6) level, and three at the moderate (PDSI $\leq$ -1.5) level. The last 3-year drought occurred at the end of the reconstruction period in 1959-1960-1961. Since 1963, the actual PDSI record (San Diego-Riverside-

Los Angeles mean) shows a severe (actual PDSI $\leq$ -3.0) 3-year drought in 1970-1971-1971 and a severe 2-year drought in 1963-64. These results suggest that droughts lasting several years have become more frequent in the past 20 years than in the previous 250 years, and that extreme drought (reconstructed PDSI $\leq$ -3.5, actual PDSI $\leq$ -4.0) has become especially more frequent in the past 20 years relative to the first half of this century.

DISCUSSION

Although the likelihood of drought is much greater in the western United States, the normally well-watered east is not immune. For instance, the northeast was severely affected by drought during 1961-1966. Thomas and Thomson (1968) reported that much of the region had PDSI values of -5.0 for more than 4 years. The drought reduced streamflow to all-time records, exhausted reservoirs and lowered groundwater levels. The effects on metropolitan supplies and agriculture are well-documented. Drought conditions returned to the northeast in 1977 and still persist in parts of the region at this writing (November, 1980).

The effects of drought on crops is more immediate in areas where natural rainfall is required to maintain adequate soil moisture. Irrigated areas are less vulnerable, the degree depending on the available surface storage and groundwater supplies. For example, the effects of the 1976-1977 drought were not nearly so severe in southern California as in other parts of the state because of the 5 million acre feet of

water imported annually from the Lower Colorado River Basin. Storage capacity in the Lower Colorado is sufficient to contain about 12½ years of the present average annual streamflow. In contrast, California reservoirs store only about one years' flow and surface supplies were soon exhausted. Cities in central and northern California resorted to extreme conservation measures and the conjunctive use of ground water for irrigated agriculture increased dramatically. An estimated 7,500 new wells were drilled in 1977, additional old wells were reactivated and others deepened (Ritschard and Tsao, 1980). The increased pumpage was largely in the Central Valley, where ground water was already being mined.

In addition to the above impacts, hydroelectric power generation by Pacific Gas and Electric was reduced from an average production of 24 billion kwh to 10 billion kwh. This 14 billion kwh deficit is roughly equivalent to 22 million barrels of oil. Fortunately the drought did not go into a third year and was broken by very heavy rains. Another year of drought would have been catastrophic.

The normally well-watered Pacific Northwest was also affected by the same drought as California, but it lasted only one year. Dry weather began in the fall of 1976 and lasted until the following fall and early winter. The 1976-77 water year was the driest on record across the Columbia River Basin. Runoff for that year, measured at the Dalles, Oregon was 78.6 million acre feet (maf), more that 52 maf below the mean annual flow and 6.3 maf lower than the previously recorded low in 1925-26. Gordon et al (1980) have presented a detailed chronology of actions taken

by the Bonneville Power Administration to meet the reduced generating capacity. By early February, 1977 a voluntary 10 percent reduction in use was asked of all customers; industrial curtailments caused electro-processing companies to reduce production and more than 500 workers were laid off. Although "brownouts" were avoided, the situation became increasingly critical and contingency plans were developed as the drought worsened. Fortunately, again, the drought did not go into a second year. Had it done so, it is difficult to visualize the resulting hardships in this region where 80 percent of the power is hydro-generated. The important point to recognize is the extreme vulnerability of this, the most water-rich region in the entire west, to a severe, yet short-duration drought.

In reality, the three factors mentioned above (surface storage, conservation and conjunctive use of ground water) are essentially the only approaches used to meet contingencies caused by drought. Of the three, only surface storage constitutes advanced planning. Conservation measures are often not applied until the situation becomes critical and are too soon forgotten once the drought is broken. Conjunctive use of ground water may or may not have deleterious effects, depending on characteristics of aquifers and capability for recharge. With better knowledge of drought recurrence and severity, contingency plans might be implemented at the onset of dry periods and thus avoid some of the consequences that result from curtailment in water usages.

The impact of drought on human populations depends on the area covered, severity, duration and the relationship between water supply and demand. As the gap between supply and demand narrows, the impacts of

droughts of a given intensity become more severe. This point is illustrated by comparing the 1930's drought with that of 1976-77. The latter covered much less area and was relatively short in duration; but it was intense and affected large population centers. It is evident that as population increases, the demand for food increases, the supply and demand curves merge and the impacts of drought can only become more and more severe. Water resources planning should give high priority to methods for alleviating drought-induced problems.

Planning for water excesses has been done for many years. Flood control structures, floodplain zoning and land management have reduced damages from floods. Drought planning, in contrast, is not very advanced. It is difficult to develop contingency measures for a product that exists in rapidly decreasing amounts. We hope that the results of our study and others like it, emphasizing that drought is not a random occurrence, but rather a regularly recurring phenomenon, will provide the background and impetus for planning to meet the inevitable water shortages that accompany periods of extended dry weather.

PART II: RELATIONSHIPS BETWEEN DROUGHT OCCURRENCE AND SOLAR VARIATION

INTRODUCTION

Many studies have been directed towards the search for periodicities in tree-ring data (Douglass 1919, 1928, 1936; Siren and Hari, 1971; LaMarche and Fritts, 1972; and Bitvinskas, 1974). In fact the origin of dendrochronology in the United States can be traced to Douglass's attempts to find evidence of solar variability in tree-ring series. The sometime existence of an approximately 22-year periodicity in tree-ring data is well documented. Douglass (1946, p. 18) noted that a periodicity of approximately 23 years was prominent in long-lived sequoias (Sequoiadendron gigantea (Lindl.) Decne.) and that "(Edmund) Schulman has found it well marked in carefully collected specimens in the intermountain (Utah) area." Douglass also noted that the period length was not constant but varied with time. In a more recent study, LaMarche and Fritts (1972), using modern statistical techniques, found that when tree-ring data were analyzed collectively on an area basis by using empirical orthogonal functions a "pair of peaks corresponding to frequencies of 22.0 and 29.2 years" appeared in the sample auto-spectrum. Although these peaks were significant at the 99 percent confidence level, they found no significance between the amplitude series of the first eigenvector of the growth (A. D. 1700-1930) and the double sunspot series when a coherence test was used.

The existence of an approximate 22-year recurrence interval for large scale drought, based on our reconstructions of 362 years of PDSI from tree-ring data, has been discussed in detail in earlier reports and

summarized here in Part I. The question logically arises as to why we were able to confirm this 22-year periodicity when others had failed to do so. The answer is probably related to the following points: (1) the tree-ring data grid differed from earlier studies, including for the first time sites east of the Rocky Mountain States; (2) the Palmer Drought Severity Index had not been used before in this kind of study; and (3) the time series analyzed for periodicity was based on the area covered by drought, regardless of where the area fell or whether or not it was continuous in space.

Inasmuch as tree-ring widths are dependent to a considerable degree upon climatic factors (e.g. especially moisture and temperature) it follows that the DAI with its near 22-year periodicity might be related to some other geophysical series with similar periodic tendencies. One that has received considerable attention in relation to the occurrence of drought is the Hale Double Sunspot Series, which has a similar periodicity (Herman and Goldberg, 1978). This relationship was reviewed by Roberts (1975). Drawing upon the work of others, he showed that there has been a tendency during the past 100 years for droughts to recur at intervals of 20-22 years in the Great Plains and that their occurrence was in phase with the Hale Double Sunspot Cycle rather than the 11-year cycle.

We have performed various statistical tests relating the DAI to the double sunspot series. These tests, in their consistency, suggest a real causal connection between large-scale drought occurrence in the western United States and long-term solar variability. Work supporting

this conclusion is discussed and summarized here. We have examined the relationships in two ways: (1) cross-spectral analysis; and (2) harmonic-dial analysis.

CROSS-SPECTRAL ANALYSIS

Cross-spectral analysis involves comparison of the two series over the entire frequency domain. The squared coherency spectrum (Figure 14) of DAI series derived from Grid S-40 versus the Hale solar cycle shows a statistically significant (95% level) peak in coherency at about 22 years. For the severe (PDSI $\leq$ -3.0) category of drought, the peak is significant at 99%.

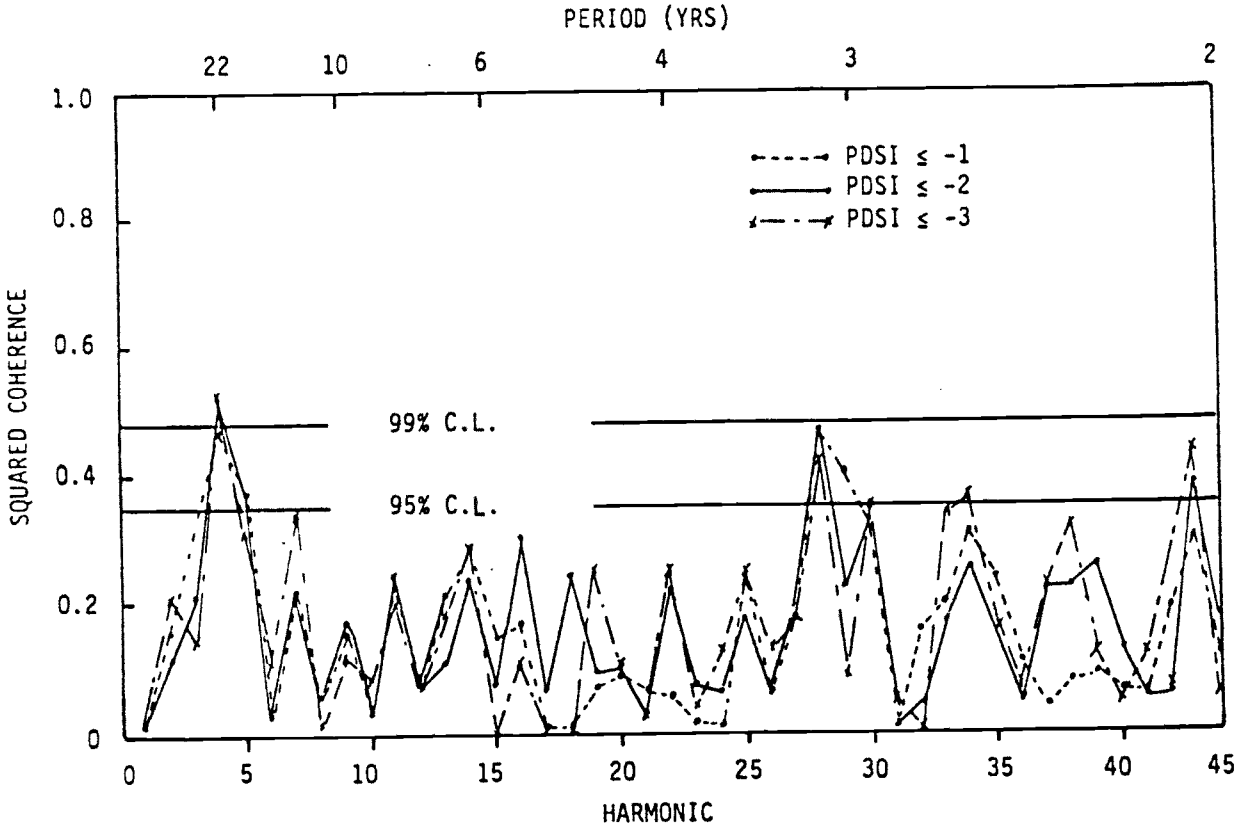

Figure 14. Coherency-squared function for drought area indices versus Hale sunspot series, A.D. 1700 to A.D. 1963.

The theoretical confidence limits shown in Figure 14 assume that each series is normally distributed, while the histograms of reconstructed DAI are appreciably skewed (Figure 15). To safeguard against the possibly invalidating effect of non-normality, we calculated empirical confidence limits independently by Monte Carlo simulations.

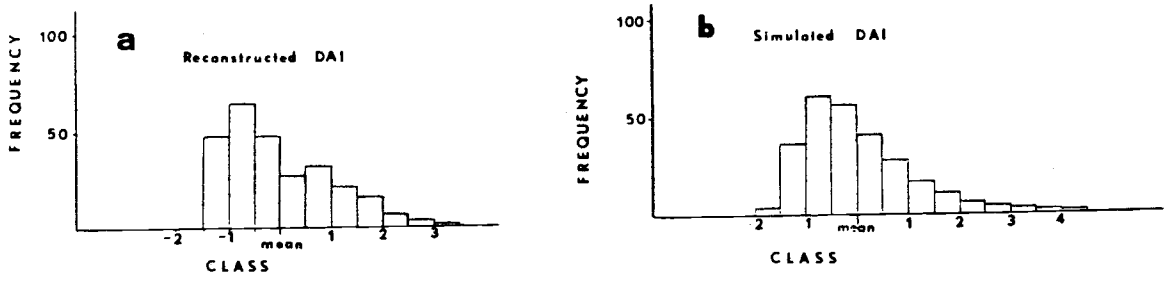

Figure 15. (a) Histogram of reconstructed (from Grid S-40) drought area index for Palmer Index $\leq$ -1.0. Ordinate is number of years of occurrence of drought index in each class interval. Class intervals are in units of 0.5 standard deviations from the mean. Total number of occurrences is 263. (b) Average histogram of 1000 simulated drought-area index series. (The histogram of the other set of 1000 simulations is virtually indistinguishable form this one and is not shown.)

This analysis was carried out on the DAI series for PDSI $\leq$ -1.0 derived from the S-40 tree-ring grid, and consisted of the following steps:

1) estimation of the probability density function and low-order persistence of the DAI series
2) modeling of the DAI series as an autoregressive-moving-average (ARMA) process, and simulation of 2000 synthetic DAI series, in two sets of 1000 each
3) Calculation of coherency-squared between each simulated DAI series and the Hale series

4) calculation of the means and standard deviations of the coherency squared for each of the two sets of 1000

5) calculation of empirical confidence intervals

Box-Jenkins modeling procedures (Box and Jenkins, 1976) were applied to the DAI series, yielding the model

$$Z_t = 0.2263\ Z_{t-1} + 7.11 + E_t$$

where Z_t and Z_{t-1} are the DAI in years t and t-1, and E_t is the randomly distributed disturbance term. The fitted model was then used to generate two sets of 1000 synthetic DAI series; the noise component, E_t, was sampled from an appropriately fit gamma distribution. The resulting average histogram of the simulated series was very similar to the histogram of the original DAI series (Figure 15), and the statistics of the simulations closely resembled those of the original series (Table 3). The simulated series are slightly more skewed and have sharper peaks than the original DAI series, but the average mean, variance, and first-order autocorrelation are well reproduced.

TABLE 3

Mean Statistics of Simulated Series and Actual Reconstructed Series

	Simulations		Actual DAI
	Set #1[1]	Set #2	
Mean	9.20	9.19	9.18
Variance	77.51	77.64	69.67
Skew	1.25	1.25	0.78
Kurtosis	5.31	5.28	2.78
Autocorrelation[2]	0.22	0.22	0.23

[1] First 1000 simulated series
[2] First order autocorrelation coefficient

Cross-spectral analysis of each simulated DAI series with the Hale series yielded 2000 coherency squared values. As before, these were analyzed in two groups of 1000 each; the means and empirical 95% confidence intervals were found for both subsets, and the results were plotted on Figure 16, along with the original coherency squared of the "actual" reconstructed DAI series with the Hale series. The coherency squared of the DAI at a period of about 22 years is significant at greater than the 95% confidence level, as it was in Figure 14, where the confidence limits were theoretical and based on the normality assumption. Therefore the statistical significance of the relationship between the Hale cycle and the DAI series appears not to be nullified by the non-normality of the DAI series.

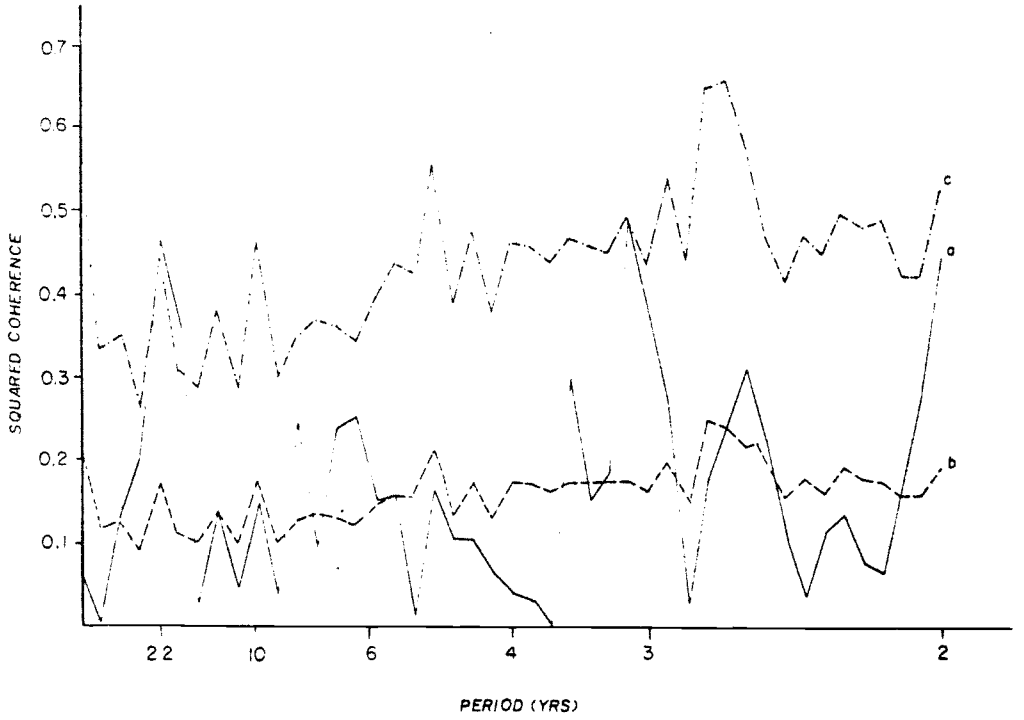

Figure 16. Results of cross-spectral analysis between simulated drought-area index series and the Hale sunspot series. (a) Coherency squared function of reconstructed (Grid S-40) DAI for PDSI $\leq$ -1.0 with Hale sunspot series. (b) Mean coherency-squared between 1000 Simulated DAI series and the Hale series. (c) Confidence limits (95%) on coherency-squared based on sample distribution of 1000 values of coherency squared between simulated DAI and the Hale series.

The relationship between the Hale series and the DAI series (for PDSI $\leq$ -1 from Grid S-40) can be seen more clearly when both series are filtered by a bandpass filter (Filter No. 1, Figure 17) and then superimposed over one another (Figure 18). This filter has a maximum response at 20.6 years, and retains only those variations in the data at frequencies corresponding to periods between roughly 15 and 31 years. Figure 18 shows that maxima in drought area have generally tended to lag behind minima in the Hale series, although the relationship appears to have broken down for some time in the late 1800's. If one assumes the nominal periodicity in the sunspot series of 22 years, a plot of DAI against years after the Hale minimum (Figure 19) shows that drought has tended to peak two years following the Hale sunspot minimum.

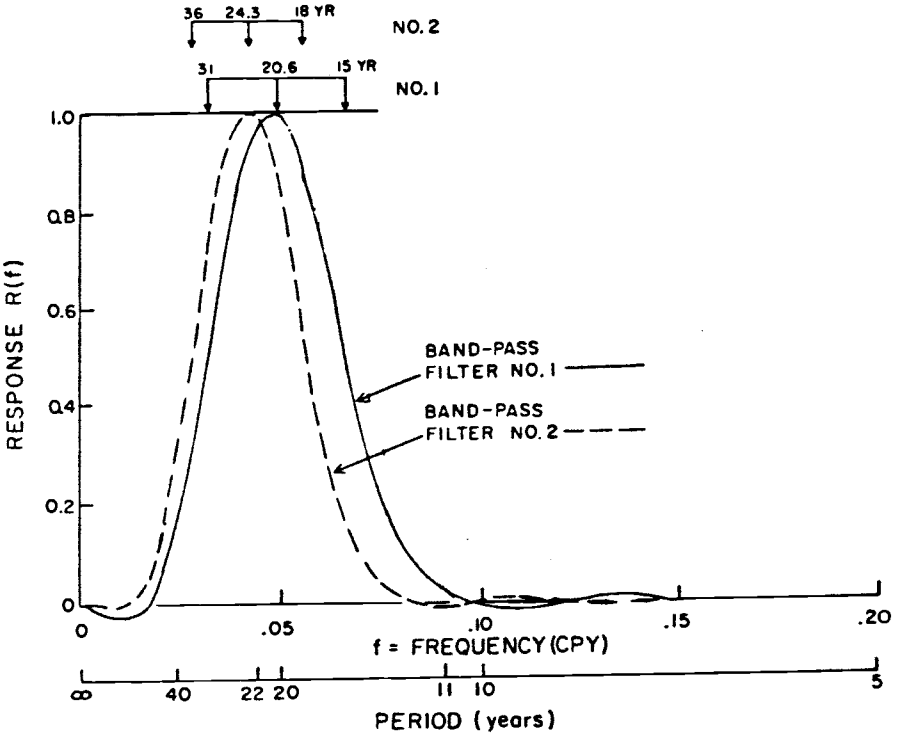

Figure 17. Response functions of bandpass filters. Peak response and half-response points are indicated for both filters at top (period in years).

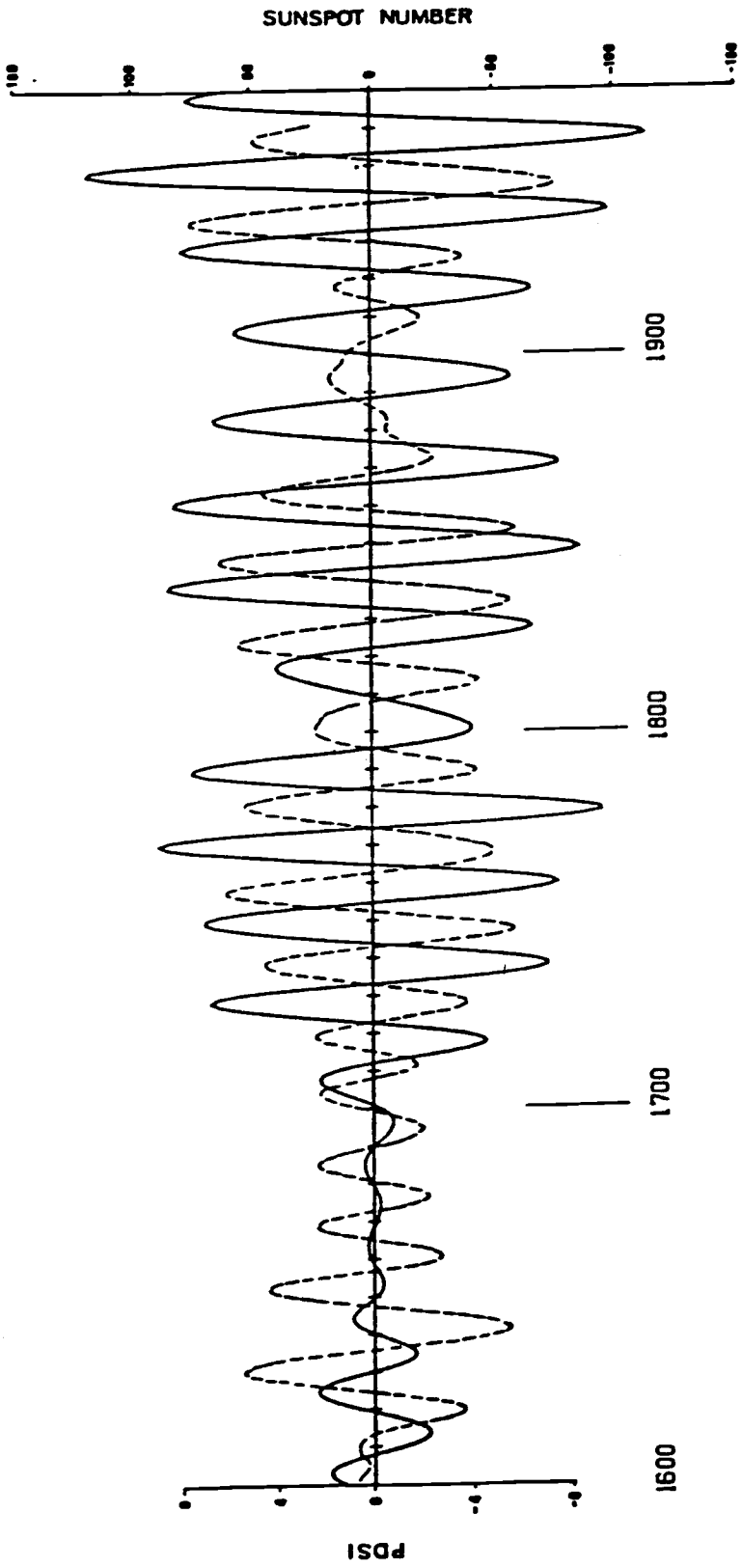

Figure 18. Filtered Hale sunspot series (solid line) and drought-area index series reconstructed from Grid S-50 (dashed line). Both series were filtered by bandpass filter #1, whose response function is shown in Figure 17.

Figure 19. Approximate total area of drought versus number of years after Hale sunspot minimum. Based on DAI series for PDSI $\leq$ -1.0 reconstructed from Grid S-40. Abscissa represents nominal number of years -- each Hale cycle was first adjusted to a common period-length of 22 years.

HARMONIC DIAL ANALYSIS

A harmonic-dial analysis (Brier, 1961) was used to further study the phase relationship between sunspots and drought. The DAI series and Hale series were first filtered by bandpass filters (two separate analyses were run, one for each filter shown in Figure 17), and the maxima from the filtered DAI series (Figure 18) were then plotted on the dial, where the plotted position for each drought peak was determined by 1) the number of years since the preceding sunspot minimum and the number of years until the following sunspot minimum, and 2) the amplitude of the DAI peak. The resulting figure (Figure 20) resembles a cluster of bullet holes in a rifle target.

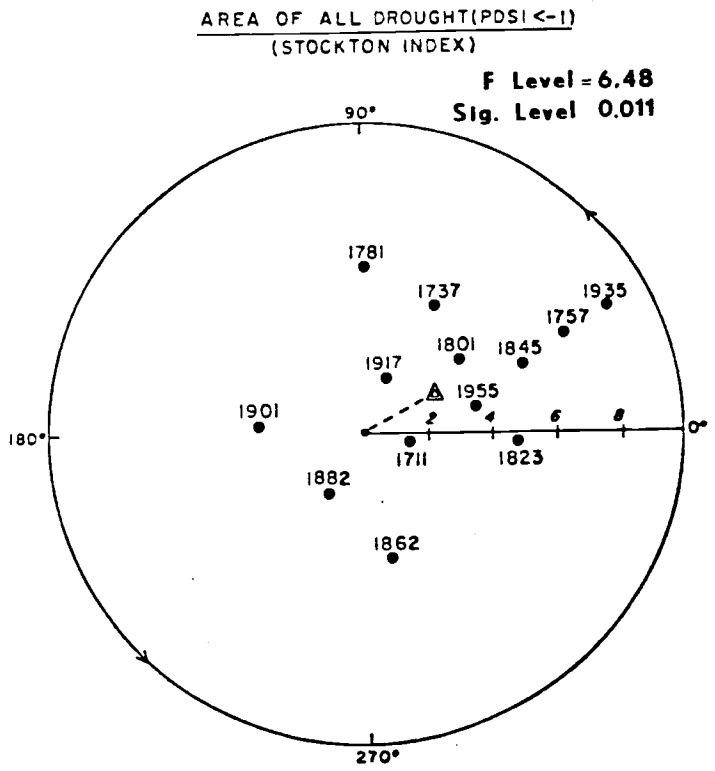

Figure 20. Harmonic dial based on reconstructed (from Grid S-40) DAI series for Palmer Index $\leq$ -1.0 and on Hale sunspot series. Series filtered before analysis by filter #1 (Figure 17). Triangle marks centroid.

The centroid of the plotted points was computed, and the strength of the phase locking between the two series was tested by an F-test. The stronger the phase locking, the greater the tendency for points to align along one particular angular direction; the greater the amplitude of a particular peak, the further it is located away from the center of the figure. Details of the analyses performed for the various grids can be found in Mitchell, Stockton and Meko (1979). In general, confidence levels were found to be greater than 99% for PDSI $\leq$ -1.0 and -2.0, 98% for PDSI $\leq$ -3.0 and 90% for PDSI $\leq$ -4.0.

Amplitude Modulation of Drought and Sunspot Series

The plot of the filtered series of DAI and sunspots (Figure 18) shows that in addition to the apparent phase locking in the 22-year rhythm, there is a similarity in amplitude modulation of the two series on the time scale of the Gleissberg cycle (≈90 years). The two highest drought peaks, 1750's and 1930's, immediately precede the two highest sunspot peaks, and the relatively low drought peaks correspond to low amplitude sunspot peaks. To test the relationship we caluclated correlation coefficients between amplitudes of drought maxima from the filtered DAI series, and the envelope of the Hale sunspot cycle at the time of the corresponding drought maxima. The individual correlation coefficients for the various series are given in Table 4.

In addition, a "weighted mean" correlation coefficient was computed between the sunspot envelope and a time series of drought maximum derived by the following steps:

TABLE 4

CORRELATION BETWEEN DROUGHT CYCLE AMPLITUDE AND ENVELOPE OF HALE SUNSPOT CYCLE*

1700 - 1962 A.D.

PDSI LIMIT	DAI FAMILY	FILTER 1			FILTER 2		
		NUMBER MAXIMA	CORRELATION COEFFICIENT	SIG. # LEVEL	NUMBER MAXIMA	CORRELATION COEFFICIENT	SIG. # LEVEL
-1	S-40	12	.645	.05	11	.548	--
	S-50	12	.683	.02	11	.685	.02
	F-65	12	.365	--	11	.209	--
-2	S-40	12	.555	--	11	.557	--
	S-50	12	.571	--	11	.554	--
	F-65	12	.550	--	12	.386	--
-3	S-40	12	.522	--	11	.554	--
	S-50	12	.544	--	11	.634	.05
	F-65	12	.555	--	11	.456	--
-4	S-40	11	.511	--	10	.506	--
	S-50	11	.770	.01	11	.776	.005
	F-65	12	.338	--	11	.371	--

*Envelope of Hale sunspot numbers filtered by Filter 1
#Two-tailed test (significance .05 or higher)

1) The maxima series for each of the 3 reconstructed series of PDSI $\leq$ -1 was rescaled to have an average value of 1. The resulting rescaled series were averaged together yielding a "mean" series for PDSI $\leq$ -1 that incorporated information from reconstructions based on all 3 tree-ring grids.
2) Step 1 was repeated for PDSI $\leq$ -2, -3 and -4 series, resulting in a 4 "mean" series.
3) A weighted average of the 4 series resulting from step 2 was computed; the largest weight was on PDSI $\leq$ -1 and the smallest on PDSI $\leq$ -4, based on the rationale that the reconstructions considered to contain the least "noise" should be weighted most heavily.

The resulting correlation coefficient was 0.71 for the drought series filtered by filter No. 1, and 0.59 for the series filtered by filter No. 2, with confidence levels of 99% and 95%, respectively.

The "weighted means" involving all PDSI limits, based on each of the two filters, are plotted in Figure 21 along with Hale sunspot cycle envelope since A.D. 1600. Some interesting conclusions are suggested by this figure. First is the tendency for the epochs of large-amplitude drought cycles to lead those of large-amplitude sunspot cycles by 10 or 20 years. Also of interest is the indication that the amplitude of the 22-year drought rhythm was quite large going into the Maunder Minimum, but that it decreased to a very low value near the end of that period (about A.D. 1700). The drought rhythm amplitude was nearly as low again around A.D. 1900. The amplitude of the Dust Bowl drought of the 1930's

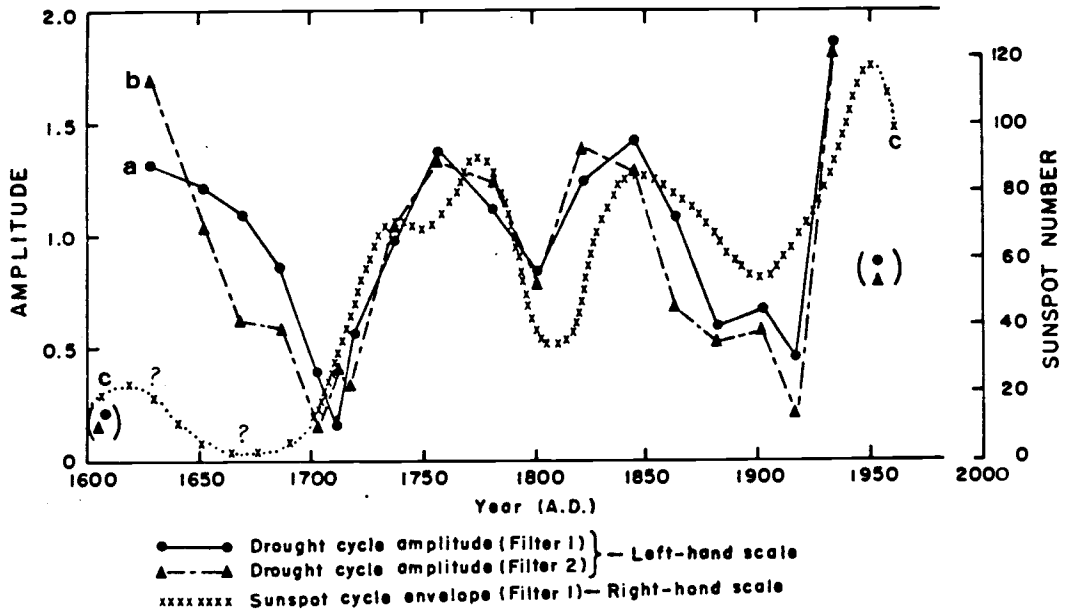

Figure 21. Amplitude modulation of DAI series and Hale sunspot series. (a) Amplitudes of maxima of "weighted mean" DAI, filtered beforehand by filter #1 (Figure 17). (b) Same series as in 'a', except filtered with filter #2. (c) Envelope of Hale sunspot series. End points of filtered drought series (in parentheses) are uncertain. Sunspot data for A.D. 1600 to A.D. 1700 are tentative reconstructions from J. Eddy.

stands out in this analysis as probably the most widespread drought event, as well as one of the most extreme events on the Palmer Index Scale since A.D. 1600 in the western U. S. It may or may not be significant that the 1930's were followed within 20 years by the highest sunspot numbers ever recorded.

We conclude that the amplitude of the 22-year drought rhythm appears to lead, by a fraction of a Hale cycle, the amplitude of the Hale sunspot cycle.

DROUGHT OUTLOOK

The results indicate that the risk of large-scale drought increases following the Hale sunspot minimum. It is important to realize that the statistically significant phase-locking between reconstructed DAI and the Hale series as shown on the harmonic dial (Figure 20) represents a small part of the total variance of drought as measured by DAI, and that other factors are often likely to mask whatever influence sunspots may have over drought. For example, the filtered DAI series for PDSI $\leq$ -1.0, from Grid S-40, retains only about 15% of the variance of the original reconstructed DAI, which itself accounted for only 72% of the variance in actual DAI during the calibration period (Table 1). It is this filtered series that is shown in Figure 18 and that was analyzed on the harmonic dial.

Another complicating factor is the temporary breakdown in the approximately two-year lag between sunspot minimum and drought maximum in the late 1800's and early 1900's, when the DAI appears to gain a full cycle on the Hale series (Figure 18). This points out that we cannot say with certainty that a drought maximum will follow within a few years of a Hale-series minimum.

We also emphasize that the DAI is an approximation of total area of drought in the western U. S. regardless of location or continuity in space. A given location in the western U. S. need not show the same periodic tendency in drought as this areal measure.

Finally, no matter how strong the relationship between drought and sunspots, drought prediction is made uncertain by the unpredictability of the Hale series itself. The period of the 11-year sunspot series has in the past ranged from 8.5 years to 16 years (Herman and Goldberg, 1978), implying that one could be in error by 5 or more years in predicting the time of the next Hale minimum.

With the previously mentioned reservations in mind, what can be said about the future likelihood of large-scale drought? A cumulative frequency plot of reconstructed DAI (Figure 22) shows that some events, particularly the worst drought years of the 1930's, were extremely rare, and are very unlikely to be equaled in, say, the next 25 years. The

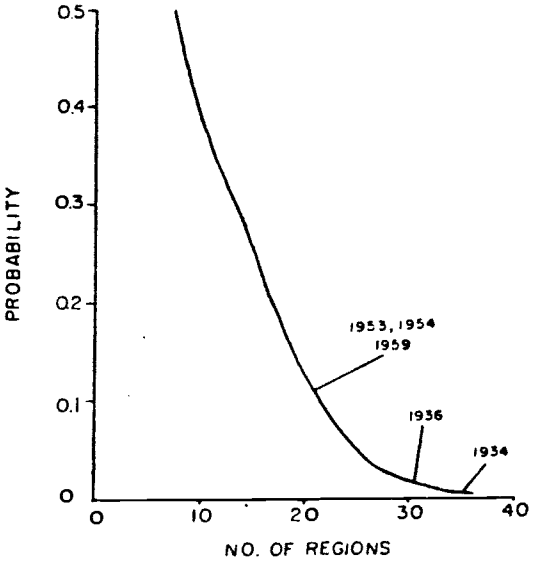

Figure 22. Cumulative frequency distribution of drought-area index (DAI) for PDSI $\leq$ -1.0 reconstructed from Grid S-40. Scale at left gives long-term empirical probability of exceeding given extent of drought as measured by DAI. Magnitude of some recent major droughts are marked on the figure.

drought of 1934, for example, stood out as the most widespread in the 263-year and the 363-year reconstructions. Figure 22 also shows that 1936 has an exceedance probability of less that 2%, and that the driest reconstructed years of the 1950's (1953, 1954 and 1959) have an exceedance probability of about 13%.

Conditional exceedance probabilities have also been computed (Figure 23) to show variations with position in time relative to the Hale sunspot minimum. In general, these plots show that the probability of exceeding a given drought tends to peak at an average of 2 years after the Hale minimum and to bottom out at about 10 to 15 years after the Hale minimum. For example, the plot for PDSI $\leq$ -1.0 from Grid S-40 shows that the probability that 10 or more regions will have PDSI $\leq$ -1.0 peaks at 50% two years after the sunspot minimum, and reaches a low of about 22% ten years after the sunspot minimum. Since the most recent Hale sunspot minimum was in 1976, these results suggest that we may now be in a period of decreasing risk of large-scale drought, with peak likelihood due back again around the year A.D. 2000, assuming the next Hale sunspot minimum occurs in A.D. 1998.

If the amplitude-modulation is also considered, the solar influences would not appear to be most favorable to large-scale drought until around A.D. 2022, under the very uncertain assumptions that the next Gleissberg maximum occurs in the 2040's ($\approx$90 years after the peak in the 1950's) and that the Hale cycle is regular over its next two time cycles with a period of 22 years. Once again, however, we emphasize that the uncertainty in the relationships studied is much too great to make operational predictions. Indeed, such predictions are unlikely until an acceptable physical cause-effect link is developed between solar variability and drought.

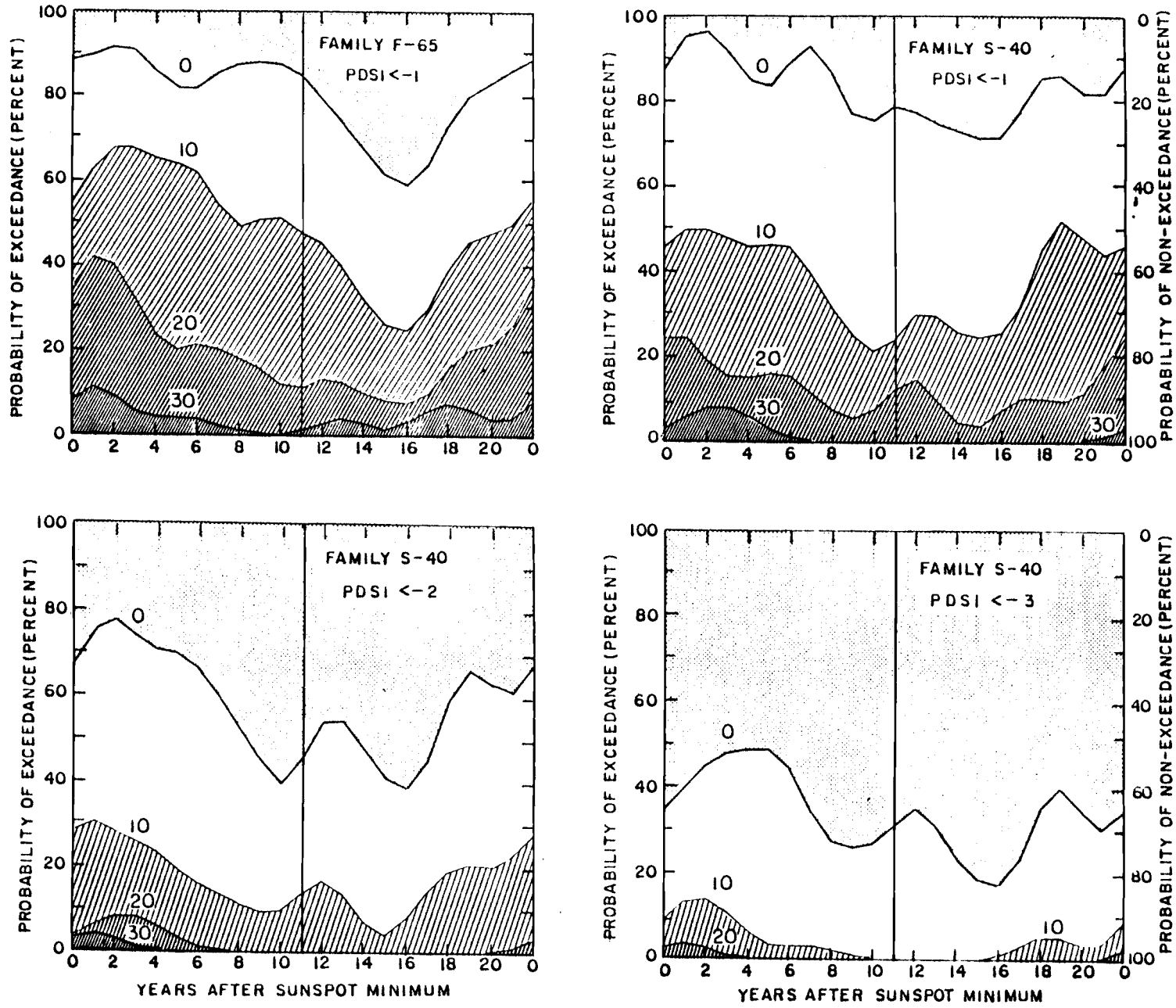

Figure 23. Conditional probabilities of exceeding various extents of drought. Plots are given for drought-area indices derived from each of four "families" (tree-ring grids), and for four extents of drought: curves labeled "0" give probability that one or more regions are in drought, plots labeled "10" that 10 or more are in drought. Abscissa gives nominal number of years after sunspot minimum -- each sunspot cycle has been rescaled to a period of 22 years.

CONCLUSION

In this report we have presented and summarized evidence that the extent of drought in the western United States varies in a periodic manner similar to the 22-year time scale of the well known Hale magnetic cycle on the sun. The level of statistical significance obtained appears sufficiently strong to encourage and justify serious investigations into the causal relationships. Indeed, we hope that our results will stimulate such inquiries regardless of whether they support or refute our conclusions.

Again, it should be emphasized that the relationships between drought and solar behavior are presently too tenuous for their use in reliable predicitions of climate. Our data simply imply that the risk of drought in unspecified regions west of the Mississippi River are appreciably greater in years following a Hale sunspot minimum than at other times during the Hale cycle. Even so, we believe that the information gained in this study can be used to great advantage in water resources planning.

LITERATURE CITED

Bitvinskas, T. T., 1974. Dendroclimatic investigations. Gidrometeoizdat, Leningrad.

Blasing, T. J., 1978. Time series and multivariate analysis in paleoclimatology. In Time Series and Ecology Processes, H. H. Shagart, Ed., pp. 213-228. Soc. for Indust. and Appl. Mathematics, Philadelphia, PA. 328 pp.

Box, G. E. P., and G. M. Jenkins, 1976. Time Series Analysis: Forecasting and Control (revised edition). Holden-Day, Inc., San Francisco, CA.

Brier, G. W., 1961. Some Statistical aspects of long-term fluctuations in solar and atmospheric phenomena. In Proceedings: Solar Variations, Climatic Change, and Related Geophysical Problems, ed. by R. W. Fairbridge. Annals of the New York Academy of Sciences, Vol. 95, Art. 1, 1-740.

Douglass, A. E., 1919. Climatic cycles and tree growth. Carnegie Institute of Washington, Pub. No. 289, Vol. 1.

_____, 1928. Climatic cycles and tree growth. Carnegie Institute of Washington, Pub. No. 289, Vol. II.

_____, 1936. Climatic cycles and tree growth. Carnegie Institute of Washington, Pub. No. 289, Vol. III.

_____, 1946. Research in dendrochronology. University of Utah Bulletin, Vol. 37, No. 2. Biological Series Vol. 10, No. 1.

Fritts, H. C., 1976. Tree Rings and Climate. Academic Press, London. 567 pp.

Fritts, H. C., Blasing, T. J., Hayden, B. P. and J. E. Kutzbach, 1971. Multivariate techniques for specifying tree growth and climatic relationships and for reconstructing anomalies in paleoclimate. J. of Appl. Meteor. 10(5):845-964.

Gordon, W. R., Watkins, C. H. and R. C. Lamb, 1980. BPA hydrologic forecasting considerations during the 1976-77 drought. In Proceedings Engineering Foundation Conf. of Improved Hydrologic Forecasting, Why and How. Pacific Grove, CA, March 25-30, 1979. ASCE, New York. pp. 274-284.

Herman, John R. and R. A. Goldberg, 1978. Sun, Weather and Climate. Scientific and Technical Information Branch, NASA, SP-426. Washington, D. C. 360 pp.

Hoyt, W. G. and W. B. Langbein, 1944. The yield of streams as a measure of climatic fluctuations. Geographical Rev. 32(2): 218-234.

Hurst, H. E., 1951. Long-term storage capacity of reservoirs. Trans. Amer. Soc. Civ. Eng. 116. p. 770.

_____, 1957. A suggested statistical model of some time series which occur in nature. Nature 180:494.

Hurst, H. E., Black, R. P. and Y. M. Simaica, 1965. Long-term Storage: an Experimental Study. Constable and Co., Ltd., London. 145 pp.

Julian, Paul R., 1970. An application of rank-order statistics to the joint spatial and temporal variations of meteorological elements. Monthly Weather Review 98(2):142-153.

Kutzbach, J. E., 1967. Empirical eigenvectors of sea level pressure, surface temperature and precipitation complexes over North America. J. Appl. Meteor. 6(5):791-802.

LaMarche, V. C., Jr. and H. C. Fritts, 1972. Tree rings and sunspot numbers. Tree-Ring Bulletin 32:21-35.

Mitchell, J. Murray, Jr., Stockton, C. W. and D. M. Meko, 1979. Evidence of a 22-year rhythm of drought in the western United States related to the Hale solar cycle since the 17th century. In Solar-Terrestrial Influences on Weather and Climate, B. M. McCormac and T. A. Seliga, eds. D. Reidel Pub. Co. Dordrecht, Holland. pp. 125-143.

Palmer, W. C., 1964. Climatic variability and crop production. Proc. of Seminar on "Weather and Food Supply". Center for Agric. and Econ. Development, Iowa State University, Ames, Iowa. CAED Report 20:173-187.

Palmer, W. C., 1965. Meteorological drought. U. S. Weather Bureau Research Paper 45. U. S. Dept. of Commerce, Washington, D. C. 58 pp.

Ritschard, R. L. and K. Tsao, 1980. Energy and water conservation strategies in irrigated agriculture. Water Resources Bull. 16(2): 340-347.

Roberts, W. O., 1975. Relation between solar activity and climate change. Goddard Space Flight Center, Special Report SP-366, NASA. W. R. Baudeen and S. P. Maran, eds. p. 13

Sirén, G and P. Hari, 1971. Coinciding periodicity in recent tree rings and glacial sediments. Rep. KEVO Subarctic Res. Sta. 8: 155-157.

Stockton, C. W. and D. M. Meko, 1975. A long-term history of drought occurrence in western United States as inferred from tree rings. Weatherwise 28(6): 244-249.

Thomas, H. E. and M. T. Thomson, 1968. Effect of the drought upon water resources of the North Atlantic Region. Proc. Fourth American Water Resources Conf., Amer. Water Resources Assoc., Minneaplois. 597-612.

Thompson, L. M., 1973. Cyclic weather patterns in the middle latitudes. J. Soil and Water Conservation 28:87-89

Thornthwaite, C. W., 1948. An approach toward a rational classification of climate. Geophysical Review 38:58-94.

Thornthwaite, C. W. and J. R. Mather, 1955. The water balance. Drexel Inst. Tech. Publ. Climatology 8(1):1-104. Centerton, N. J.

Trewatha, Glenn T., 1961. The Earth's Problem Climates. University of Wisconsin Press, Ltd. Madison. 334 pp.

Willett, H. C., 1965. Solar-climatic relationships in the light of standardized climatic data. J. Atmos. Sci. 22:120.